

DISCRETE EXTREMAL LENGTHS  
OF GRAPH APPROXIMATIONS  
OF SIERPIŃSKI CARPETS

by

Robert Jason Malo

A dissertation submitted in partial fulfillment  
of the requirements for the degree

of

Doctorate of Philosophy

in

Mathematics

MONTANA STATE UNIVERSITY  
Bozeman, Montana

May 2015

©COPYRIGHT

by

Robert Jason Malo

2015

All Rights Reserved

## TABLE OF CONTENTS

1	CONFORMAL DIMENSION . . . . .	<b>1</b>
1.1	Introduction and Basic Examples . . . . .	1
1.2	Hausdorff Dimension . . . . .	4
1.3	Quasisymmetric Maps and Conformal Dimension . . . . .	9
1.4	Graph Approximations and Modulus . . . . .	17
1.5	Graph Approximation of the Sierpiński Carpet . . . . .	22
2	ALGORITHM FOR EXTREMAL LENGTH . . . . .	<b>31</b>
2.1	Combinatorics of the Standard Graph Approximations . . . . .	31
2.2	Extremal Length in Graphs . . . . .	35
2.3	The Algorithm . . . . .	40
3	RESULTS . . . . .	<b>53</b>
3.1	Implementation . . . . .	53
3.2	Visual Representations of the Algorithm . . . . .	58
3.3	Numerical Results . . . . .	58
3.4	Summary of Data . . . . .	71
	REFERENCES CITED . . . . .	<b>75</b>

## LIST OF TABLES

Table		Page
3.1	Computed $\hat{l}_n$ values for $p = 1.75$ in $A_2$ . . . . .	67
3.2	$A_2$ extrapolations . . . . .	70
3.3	$A_3$ extrapolations . . . . .	70
3.4	Projected length values for $A_2, A_3,$ and $A_4,$ iterations 501-5000 . . . .	71
3.5	Projected length values for $A_2, A_3,$ and $A_4,$ iterations 4501-5000 . . .	72
3.6	Projected length for $p = 1.70$ . . . . .	73
3.7	Projected length for $p = 1.80$ . . . . .	73
3.8	Projected length for $p = 1.75$ . . . . .	74

## LIST OF FIGURES

Figure	Page
1.1 Middle third Cantor set . . . . .	2
1.2 von Koch curve . . . . .	2
1.3 Sierpiński gasket . . . . .	3
1.4 Sierpiński carpet . . . . .	3
1.5 Hausdorff measure . . . . .	5
1.6 Open set condition for the von Koch curve . . . . .	7
1.7 Construction of the Sierpiński carpet . . . . .	23
1.8 Graph approximations of the Sierpiński carpet . . . . .	24
1.9 Covering graph of the Sierpiński carpet . . . . .	25
1.10 Detours in a Sierpiński lattice. . . . .	26
1.11 Reflecting a curve in $G_{N+n}^c$ . . . . .	29
2.1 Embeddings of $A_n$ into $A_{n+1}$ . . . . .	32
2.2 Graph approximations of the Sierpiński carpet . . . . .	33
2.3 Minimal horizontal separating sets . . . . .	35
2.4 The linear approximation of $(\cdot)^{p-1}$ based at $x$ . . . . .	43
3.1 Construction of $A_2^*$ . . . . .	55
3.2 A path generated by a minimal $m$ -dual-length separating set . . . . .	57
3.3 Mass distribution under iteration on $A_4$ . . . . .	59
3.4 Mass distribution on $A_2$ and $A_3$ . . . . .	60
3.5 Mass distribution on $A_4$ for $p = 1.70$ . . . . .	61
3.6 Mass distribution on $A_4$ for $p = 1.75$ . . . . .	62
3.7 Mass distribution on $A_4$ for $p = 1.80$ . . . . .	63
3.8 Mass distribution on $A_5$ for $p = 1.70$ . . . . .	64

## LIST OF FIGURES - CONTINUED

Figure	Page
3.9 Mass distribution on $A_5$ for $p = 1.75$ . . . . .	65
3.10 Mass distribution on $A_5$ for $p = 1.80$ . . . . .	66
3.11 $A_2$ data fitting for iterations 2-5000 . . . . .	68
3.12 $A_2$ data fitting for iterations 501-5000 . . . . .	68

## ABSTRACT

The study of mathematical objects that are not smooth or regular has grown in importance since Benoit Mandelbrot's foundational work in the late 1960s. The geometry of fractals has many of its roots in that work. An important measurement of the size and structure of fractals is their dimension. We discuss various ways to describe a fractal in its canonical form. We are most interested in a concept of dimension introduced by Pierre Pansu in 1989, that of the conformal dimension. We focus on an open question: what is the conformal dimension of the Sierpiński carpet?

In this work we adapt an algorithm by Oded Schramm to calculate the discrete extremal length in graph approximations of the Sierpiński carpet. We apply a result by Matias Piaggio to relate the extremal length to the Ahlfors-regular conformal dimension. We find strong numeric evidence suggesting both a lower and upper bound for this dimension.

## CONFORMAL DIMENSION

In 1967 Benoit Mandelbrot [Man67] published a foundational essay on the topic of fractal geometry. In the decades since, the mathematical study of fractals has been an area of significant interest. In this chapter we use four standard examples to build much of the basic theory of fractals. In particular, we look closely at various notions of dimension. The centrality of dimension in fractal geometry is evidenced by the fact that Mandelbrot originally introduced the term fractal to denote an object that has a Hausdorff dimension strictly larger than its topological dimension. We consider those classical ideas of dimension and a notion of dimension introduced by Pierre Pansu in 1989, the conformal dimension.

### 1.1 Introduction and Basic Examples

We begin by discussing four elementary examples that will give us a framework for the upcoming discussion. The examples are classic constructions that date from the late nineteenth and early twentieth century.

One of the simplest fractals to construct is the middle third Cantor set, named for the German mathematician Georg Cantor, see Figure 1.1. Let  $K_0$  be the unit interval  $[0, 1]$ . Remove the open middle third  $(1/3, 2/3)$  to obtain  $K_1 = [0, 1/3] \cup [2/3, 1]$ . Removing the open middle third of each remaining interval gives  $K_2 = [0, 1/9] \cup [2/9, 1/3] \cup [2/3, 7/9] \cup [8/9, 1]$ . Continuing in this manner, we construct a decreasing sequence of compact sets  $\{K_i\}_{i \geq 0}$  and obtain the middle third Cantor set

$$K := \bigcap_{i=0} K_i$$

It will be useful in the future to view the construction at each step not as removing intervals, but rather as replacing each previous interval with two intervals of one third

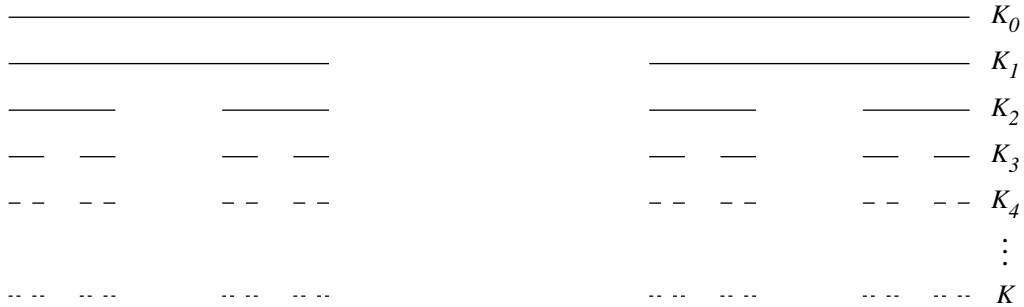


Figure 1.1: Middle third Cantor set

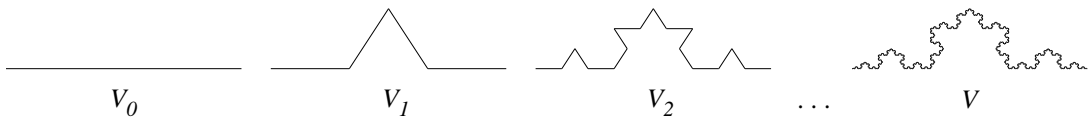


Figure 1.2: von Koch curve

the length. We will do so explicitly in the following section.

The second example we consider is the von Koch curve, often called a snowflake curve, named after the Swedish mathematician Helge von Koch. While the Cantor set removed an interval at each iteration, the von Koch curve replaces each middle third with two segments of the same length. In essence, replacing a segment with the two other sides of an equilateral triangle. Alternatively, we can view the construction as replacing each interval with four intervals of one third the length, see Figure 1.2.

Allowing  $V_0 = [0, 1]$  as we did with the Cantor set, we have at each iteration  $V_k$  the length of the curve is  $(4/3)^k$  so that the limiting object, the von Koch curve  $V$ , has infinite length. Nonetheless, the curve has zero area in the plane. It will be useful to find a measure of the size of this curve, and similar objects, that is a more useful measurement than infinite length or zero area. One such measure of size is the dimension, which we will discuss in detail soon. However, two additional examples

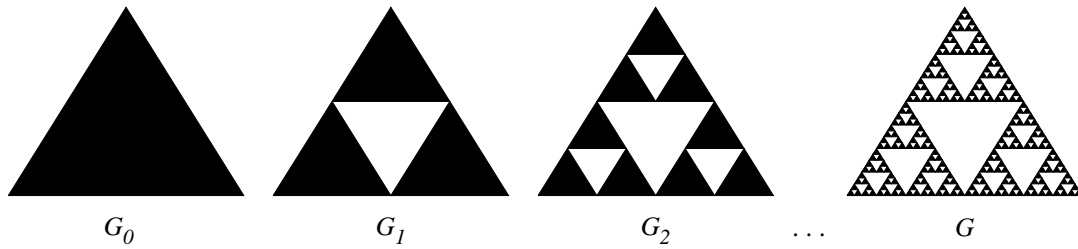


Figure 1.3: Sierpiński gasket

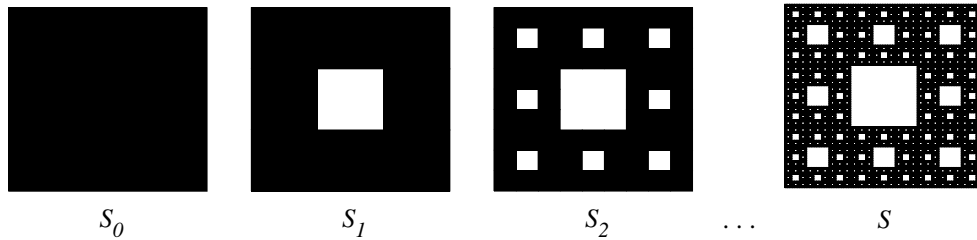


Figure 1.4: Sierpiński carpet

are worth familiarizing ourselves with before we dive in.

The final two examples are similar to the construction of the Cantor set and both due to the Polish mathematician Waclaw Sierpiński. The Sierpiński gasket is constructed from an equilateral triangle. At each iteration we divide the triangle, or triangles, into four congruent subtriangles and remove the central subtriangle, see Figure 1.3. A Sierpiński carpet is constructed from a square. At each iteration we divide the square, or squares, into nine congruent subsquares and remove the central subsquare, see Figure 1.4. The Sierpiński carpet will be focus of much of the following, we will return to it with a formal construction in the following chapter.

A routine geometric series argument shows that the area of the carpet is zero. Assuming that we start with a unit square, we have  $1 - (1/9 + 8/81 + \dots) = 1 - \sum_{k=0}^{\infty} (1/9)(8/9)^k = 0$ . A similar argument shows the gasket also has zero area. Again we see that area is a poor measure of these objects. A more useful analytic tool for

these types of fractals is their dimension. One such notion of dimension is Hausdorff dimension which we will define now.

## 1.2 Hausdorff Dimension

Traditional measurements such as length and area fail to adequately describe fractals. A central tool for their study is the notion of dimension, roughly speaking, a measure of how much space a fractal occupies at each scale. There are many ways to quantify the dimension, see for example Falconer [Fal03, Chapter 3]. For our examples, all common notions of fractal dimension coincide. The notions of topological dimension and conformal dimension that we address in future sections will differ however.

We will use the definition of Hausdorff, based on a construction of Carathéodory. Although Hausdorff dimension is rigorous in the sense that it is defined for all sets and built from measures which are well understood, it is often difficult to compute explicitly or even estimate computationally. However, it is fundamental to the field and our subsequent discussion. In the following definition, and many of the subsequent statements, we will write  $|U|$  to represent the diameter of  $U$ , i.e.  $|U| = \sup\{d(x, y) : x, y \in U\}$ .

**Definition 1.2.1.** Let  $(X, d)$  be a metric space and  $s > 0$ . For  $\delta \in (0, \infty]$  we define

$$\mathcal{H}_\delta^s(X) := \inf \left\{ \sum_{i=1}^{\infty} |U_i|^s : X \subseteq \bigcup_{i=1}^{\infty} U_i \text{ and } |U_i| < \delta \right\}$$

and

$$\mathcal{H}^s(X) := \lim_{\delta \rightarrow 0} \mathcal{H}_\delta^s(X).$$

$\mathcal{H}^s$  is the  $s$ -dimensional **Hausdorff measure**, and  $\mathcal{H}_\infty^s$  is the  $s$ -dimensional **Haus-**

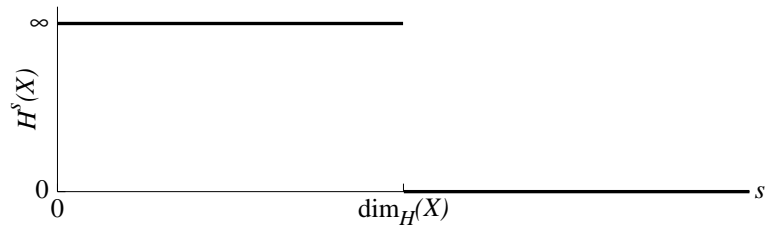


Figure 1.5: The Hausdorff dimension is the value of  $s$  where the measure changes from  $\infty$  to 0.

**dorff content.** The **Hausdorff dimension** of  $X$  is defined as

$$\dim_H(X) := \inf\{s > 0 : \mathcal{H}^s(X) = 0\}.$$

The Hausdorff dimension is the critical exponent where the Hausdorff measure changes from  $\infty$  to 0, so an alternative definition is

$$\dim_H(X) = \sup\{s > 0 : \mathcal{H}^s(X) = \infty\}.$$

An additional characterization of the Hausdorff dimension via the Hausdorff content is

$$\dim_H(X) = \inf\{s > 0 : \mathcal{H}_\infty^s(X) = 0\}.$$

This final characterization will prove useful in Lemma 1.3.9.

Although Hausdorff dimension is typically difficult to compute, many classic fractals are generated by an iterated function system which makes their Hausdorff dimension easier to compute. In particular, the four examples in the previous section are all examples that can be generated by an iterated function system.

**Definition 1.2.2.** For a closed  $D \subset \mathbb{R}^n$ , a mapping  $S : D \rightarrow D$  is called a **contraction** if there exists a ratio  $0 < c < 1$  so that  $|S(x) - S(y)| \leq c|x - y|$  for all  $x, y \in D$ .

In the case of equality for all  $x, y \in D$ , we say  $S$  is a **contracting similarity**. A family of contractions  $\{S_1, S_2, \dots, S_m\}$  with  $m \geq 2$  is called an **iterated function system**. A non-empty compact subset  $F$  of  $D$  is called an **attractor** for the iterated function system if

$$F = \bigcup_{i=1}^m S_i(F).$$

As an example, the middle third Cantor set is the attractor of the system with  $D = [0, 1]$  and contracting similarities given by

$$S_1(x) = \frac{x}{3}; \quad S_2(x) = \frac{2+x}{3}.$$

Similarly, the Sierpiński carpet is the attractor of the system with  $D = [0, 1]^2$  and eight contracting similarities given by

$$\begin{aligned} S_1(x, y) &= \left(\frac{x}{3}, \frac{y}{3}\right); & S_2(x, y) &= \left(\frac{1+x}{3}, \frac{y}{3}\right); \\ S_3(x, y) &= \left(\frac{2+x}{3}, \frac{y}{3}\right); & S_4(x, y) &= \left(\frac{x}{3}, \frac{1+y}{3}\right); \\ S_5(x, y) &= \left(\frac{2+x}{3}, \frac{1+y}{3}\right); & S_6(x, y) &= \left(\frac{x}{3}, \frac{2+y}{3}\right); \\ S_7(x, y) &= \left(\frac{1+x}{3}, \frac{2+y}{3}\right); & S_8(x, y) &= \left(\frac{2+x}{3}, \frac{2+y}{3}\right). \end{aligned}$$

For a more extensive background and bibliography on iterated function systems see Falconer [Fal03, Chapter 9]. We present two classic theorems that further our discussion.

**Theorem 1.2.3** (Falconer, Theorem 9.1). *An iterated function system given by the contractions  $\{S_1, S_2, \dots, S_m\}$  on  $D \subset \mathbb{R}^n$  has a unique attractor  $F \subset D$ , i.e. a*

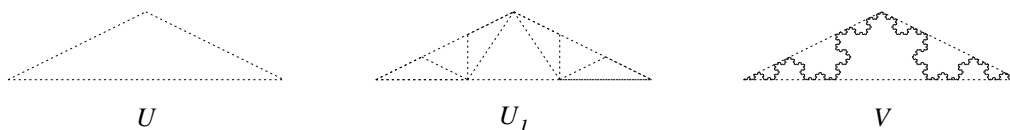


Figure 1.6: The open set  $U$  needed in the open set condition for the von Koch curve, the four images of  $U$  under the contracting similarities  $U_1 = \bigcup_{i=1}^4 S_i(U) \subset U$ , and the curve  $V$  in comparison to  $U$ .

*non-empty compact set with*

$$F = \bigcup_{i=1}^m S_i(F).$$

In order to correctly compute the Hausdorff dimension of the attractor of an iterated function system, we require the contractions to be 'basically disjoint'. Specifically, we say the contractions  $S_i$  satisfy the **open set condition** if there exists a non-empty open bounded set  $U$  so that

$$U \supset \bigcup_{i=1}^m S_i(U) \tag{1.2.1}$$

is a disjoint union.

The examples we have seen all satisfy the open set condition. For the Cantor set, we can take  $U = (0, 1)$ . For the gasket we take  $U$  to be the interior of the initial triangle and for the carpet we can take  $V$  to be the interior of the initial square. For the von Koch curve constructed from the initial segment  $[0, 1]$  we use the open triangle with vertices  $(0, 0)$ ,  $(1/2, \sqrt{3}/6)$ , and  $(1, 0)$ , see Figure 1.6.

Moran [Mor46] showed that iterated function systems that satisfy the open set condition have simply computed Hausdorff dimension.

**Theorem 1.2.4** (Moran). *Suppose the open set condition (1.2.1) holds for the con-*

tracting similarities  $S_i$  with ratios  $0 < c_i < 1$  for  $1 \leq i \leq m$ . If  $F$  is the attractor of the iterated function system  $\{S_1, S_2, \dots, S_m\}$ , then  $\dim_H F = s$ , where  $s$  is given by

$$\sum_{i=1}^m c_i^s = 1.$$

In the case where the contracting similarities each have the same ratio, we have a convenient representation for the dimension.

**Corollary 1.2.5.** *Suppose the open set condition (1.2.1) holds for the contracting similarities  $S_i$  each with ratio  $0 < c < 1$  for  $1 \leq i \leq m$ . If  $F$  is the attractor of the iterated function system  $\{S_1, S_2, \dots, S_m\}$ , then*

$$\dim_H F = \frac{\log m}{-\log c}.$$

With this corollary available, it is now clear that the Cantor set has Hausdorff dimension  $\log 2 / \log 3 \approx 0.6309$ , the von Koch curve has Hausdorff dimension  $\log 4 / \log 3 \approx 1.2619$ , the Sierpiński gasket has Hausdorff dimension  $\log 3 / \log 2 \approx 1.5850$ , and the Sierpiński carpet has Hausdorff dimension  $\log 8 / \log 3 \approx 1.8928$ . It is worth pausing to note that the construction of both the Cantor set and the von Koch curve began with a unit interval of Hausdorff dimension one. In the case of the Cantor set the dimension shrunk while in the case of the von Koch curve the dimension grew.

The Hausdorff dimension for many fractals is known, or has been computationally estimated<sup>1</sup>. Beyond mathematical constructs, physical objects from cauliflower to the coastline of England have been approximated experimentally [Man67]. Hausdorff dimension is fairly well understood for many things. However, a natural question

---

<sup>1</sup>There are around 115 items on the Wikipedia page *List of fractals by Hausdorff dimension*.

arises. If we allow the fractal to be distorted in a controlled manner, how can the Hausdorff dimension change? We begin answering this question in the next section.

### 1.3 Quasisymmetric Maps and Conformal Dimension

**Definition 1.3.1.** Let  $(X, d)$  and  $(\tilde{X}, \tilde{d})$  be metric spaces and let  $L \geq 1$ . A homeomorphism  $f : X \rightarrow \tilde{X}$  is said to be **L-bi-Lipschitz** if

$$\frac{1}{L}d(x, y) \leq \tilde{d}(f(x), f(y)) \leq Ld(x, y)$$

for all  $x, y \in X$ . We say a function is **bi-Lipschitz** if it is L-bi-Lipschitz for some finite  $L$ .

A bi-Lipschitz homeomorphism preserves Hausdorff dimension of a metric space [MT10, Corollary 1.4.18]. However, if we allow arbitrary homeomorphisms, the Hausdorff dimension of the image can change dramatically. One way we can characterize the change in the Hausdorff dimension is by considering the topological dimension (or small inductive dimension).

**Definition 1.3.2.** For a metric space  $(X, d)$  define the **topological dimension** as follows:

$$\dim_T \emptyset = -1$$

and  $\dim_T X \leq n$  if  $X$  has a basis of sets  $\{A_i\}$  whose boundaries satisfy  $\dim_T \partial A_i \leq n - 1$ .

A totally disconnected metric space has topological dimension zero. A line segment has topological dimension one since there is a neighborhood about each point with boundary of disconnected points. In general,  $\dim_T \mathbb{R}^N = N$ . We note that the topological dimension takes integer values, or infinity.

It is also worth relating the topological dimension and the Hausdorff dimension of a metric space  $(X, d)$ . Although the relationship is mentioned in passing in a number of sources, it seems to originate in Hurewicz and Wallman[HW41].

**Theorem 1.3.3** (Hurewicz and Wallman, Corollary to Theorem VII 5). *For a metric space  $(X, d)$  we have*

$$\dim_T(X, d) = \inf \left\{ \dim_H(\tilde{X}, \tilde{d}) : (\tilde{X}, \tilde{d}) \text{ is homeomorphic to } (X, d) \right\}. \quad (1.3.1)$$

**Corollary 1.3.4.** *For a metric space  $(X, d)$  we have*

$$\dim_T X \leq \dim_H X. \quad (1.3.2)$$

If we consider our previous examples, we have that the topological dimension of the middle third Cantor set is zero and the topological dimension of the von Koch curve, the Sierpiński gasket, and the Sierpiński carpet are each one. Although we have gained some measure of the underlying structure, we have lost a great deal of the subtleties of each. We would like a class of homeomorphisms that is less restrictive than bi-Lipschitz homeomorphisms, but more restrictive than an arbitrary homeomorphism. One appropriate middle ground is a quasisymmetric homeomorphism.

**Definition 1.3.5.** Given an increasing homeomorphism  $\eta : [0, \infty) \rightarrow [0, \infty)$ , a homeomorphism  $f$  between metric spaces  $(X, d)$  and  $(\tilde{X}, \tilde{d})$  is  $\eta$ -**quasisymmetric** if for distinct  $x, y, z \in X$

$$\frac{\tilde{d}(f(x), f(y))}{\tilde{d}(f(x), f(z))} \leq \eta \left( \frac{d(x, y)}{d(x, z)} \right).$$

Further, a homeomorphism  $f$  is **quasisymmetric** if it is  $\eta$ -quasisymmetric for some  $\eta$ . Two metric spaces  $(X, d)$  and  $(\tilde{X}, \tilde{d})$  are **quasisymmetrically equivalent** if there

exists a quasisymmetric map between them. In this case, we will write  $(X, d) \underset{QS}{\sim} (\tilde{X}, \tilde{d})$ .

Quasisymmetric maps are a natural replacement of quasiconformal maps in general metric spaces, and a natural generalization of conformal maps between Riemann surfaces. In Euclidean space of dimension greater than one, quasisymmetric maps coincide with quasiconformal maps.

**Lemma 1.3.6.** *Let  $(X, d)$  be a metric space and  $\varepsilon \in (0, 1)$ . Then  $d^\varepsilon(x, y) = d(x, y)^\varepsilon$  is a metric on  $X$ .*

*Proof.* The only non-trivial property to check is the triangle inequality. This follows easily using the concavity of  $g(t) = t^\varepsilon$  on  $[0, \infty)$ , which implies for all  $a, b \geq 0$ :

$$a^\varepsilon + b^\varepsilon \geq \frac{a}{a+b}(a+b)^\varepsilon + \frac{b}{a+b}(a+b)^\varepsilon = (a+b)^\varepsilon$$

Applying this with  $a = d(x, y)$  and  $b = d(y, z)$  and using the original triangle inequality gives

$$d(x, y)^\varepsilon + d(y, z)^\varepsilon \geq (d(x, y) + d(y, z))^\varepsilon \geq d(x, z)^\varepsilon$$

□

**Definition 1.3.7.** We will denote the metric space  $(X, d^\varepsilon)$  by  $X^\varepsilon$  and call it the  $\varepsilon$ -snowflake of  $X$ .

**Lemma 1.3.8.** *The map  $f : X \rightarrow X^\varepsilon$  defined by  $f(x) = x$  is quasisymmetric with  $\eta(t) = t^\varepsilon$ .*

*Proof.* This is immediately evident from the definitions. In fact, the required inequality is an equality in this case. □

**Lemma 1.3.9.** *The Hausdorff dimension of the  $\varepsilon$ -snowflake of  $X$  is  $\dim_H X^\varepsilon = \varepsilon^{-1} \dim_H X$  for all  $\varepsilon \in (0, 1)$ .*

*Proof.* It is most convenient to use Hausdorff content here. Obviously, any covering of  $X$  is a covering of  $X^\varepsilon$  and vice versa. For any such covering  $X \subseteq \bigcup_{i=1}^\infty U_i$  and for any  $s > 0$  we have

$$\sum_{i=1}^\infty |U_i|^s = \sum_{i=1}^\infty (|U_i|^\varepsilon)^{s/\varepsilon}$$

Since  $|U_i|$  is the diameter of  $U_i$  in  $X$ , and  $|U_i|^\varepsilon$  is the diameter of  $U_i$  in  $X^\varepsilon$ , taking the infimum over all covers we get

$$\mathcal{H}_\infty^s(X) = \mathcal{H}_\infty^{s/\varepsilon}(X^\varepsilon)$$

which implies the claim. □

Since  $X^\varepsilon$  is quasisymmetrically equivalent to  $X$ , this lemma shows that for any metric space  $X$  with non-zero Hausdorff dimension the supremum of dimensions of quasisymmetrically equivalent spaces is infinite. However, the infimum of these dimensions is an interesting invariant, introduced by Pansu in [Pan89].

**Definition 1.3.10.** For a metric space  $(X, d)$  define the **conformal dimension** as

$$\dim_{\mathcal{C}}(X, d) = \inf \left\{ \dim_H(\tilde{X}, \tilde{d}) : (\tilde{X}, \tilde{d}) \underset{QS}{\sim} (X, d) \right\}$$

It is clear by definition and Theorem 1.3.3 that the inequality (1.3.2) can be extended to

$$\dim_T X \leq \dim_{\mathcal{C}} X \leq \dim_H X. \tag{1.3.3}$$

**Definition 1.3.11.** A metric space  $(X, d)$  is **minimal for conformal dimension**

if

$$\dim_H X = \dim_C X$$

It will be useful to consider a few examples to get a feel for conformal dimension before we continue on.

For  $N \geq 1$ ,  $\dim_C \mathbb{R}^N = N$ . In general, for any metric space  $X$  that has topological dimension and Hausdorff dimension that agree, that metric space is minimal for conformal dimension. This follows directly from (1.3.3).

The middle third Cantor set  $K$  has an easy to compute conformal dimension. We begin by generalizing the construction of the Cantor set to rescale by a factor of  $\lambda$  instead of a factor of  $1/3$  where  $0 < \lambda < 1/2$ . By Corollary 1.2.5 we have  $\dim_H K_\lambda = \log 2 / (-\log \lambda) \rightarrow 0$  as  $\lambda \rightarrow 0$ . There exists a natural quasisymmetric map between  $K$  and  $K_\lambda$ , allowing us to conclude that  $\dim_C K = 0$ . It is worth noting that the infimum is not achieved however.

Since the von Koch snowflake curve  $V$  is the reason  $X^\varepsilon$  in Definition 1.3.7 is called the snowflake of  $X$ , it is comforting to note that  $(V, d_{eucl})$  is bi-Lipschitz equivalent to  $([0, 1], d_{eucl}^\alpha)$  where  $\alpha = \log 3 / \log 4$  [MT10]. We conclude that  $\dim_C V = \dim_C [0, 1] = 1$ .

The remaining examples are more difficult. Tyson and Wu, and earlier Laakso, [TW06] have shown that the conformal dimension of the Sierpiński gasket is one. The conformal dimension of the Sierpiński carpet is an open problem; one which we partially address in the final chapter. There are some results which will prove useful for the discussion.

Initially we note that conformal dimension, in fact all notions of dimension that

we discuss, are monotone:

$$\dim A \leq \dim B \quad \text{whenever } A \subset B.$$

Hausdorff dimension is countably stable:

$$\dim_H \left( \bigcup_i^\infty A_i \right) = \sup_i \dim_H A_i \quad A_i \in X \text{ for all } i.$$

However, conformal dimension is not even finitely stable. There exist  $S_1, S_2$  subsets of  $[0, 1]$  each with conformal dimension zero but  $S_1 \cup S_2 = [0, 1]$  which has conformal dimension one. The construction is based off an example by Tukia [Tuk89] and can be found in [MT10, Example 5.2.1]. One crucial part of the argument is an application of a theorem of Kovalev [Kov06] which is worth considering.

**Theorem 1.3.12** (Kovalev). *For a metric space  $(X, d)$*

$$\dim_c X \in \{0\} \cup [1, \infty].$$

Tyson has shown that there exist metric spaces with conformal dimension  $Q$  for all  $Q \geq 1$  [Tys00]. We have already seen that the middle third Cantor set has conformal dimension zero, so Kovalev's result is sharp.

A theorem by Bishop and Tyson [BT01] gives us a lower bound for the conformal dimension of the Sierpiński carpet.

**Theorem 1.3.13** (Bishop-Tyson). *For every compact set  $Y \subset \mathbb{R}^N$ ,  $Z = Y \times [0, 1]$  is minimal for conformal dimension.*

Since the Sierpiński carpet has the middle third Cantor set cross the unit interval as a subset, we have the following corollary.

**Corollary 1.3.14.** *For the Sierpiński carpet  $S$  the conformal dimension is bounded by*

$$1.6309\dots \approx 1 + \frac{\log 2}{\log 3} \leq \dim_{\mathcal{C}} S.$$

It is conjectured the lower bound is a strict inequality, but this remains an open question. A result from Keith and Laakso [KL04] provides strict inequality for the upper bound

$$\dim_{\mathcal{C}} S < \dim_H S = \frac{\log 8}{\log 3} \approx 1.8927\dots .$$

A construction by Kigami [Kig14] provides a slightly better upper bound.

**Theorem 1.3.15** (Kigami, Corollary 6.6). *For the Sierpiński carpet  $S$  the conformal dimension is bounded by*

$$\dim_{\mathcal{C}} S \leq \frac{\log\left(\frac{9+\sqrt{41}}{2}\right)}{\log 3} \approx 1.8581\dots .$$

In the final chapter we will present numerical evidence suggesting that

$$\dim_{\mathcal{C}} S < 1.80.$$

In fact we will make a stronger conjecture for a variation of the concept of conformal dimension called Ahlfors-regular conformal dimension, which we explain below.

For metric spaces with a self-similar structure, we can make use of that structure. One way to measure the homogeneity or regularity of a space is with Ahlfors-regularity. Roughly speaking, a metric space with an appropriate measure is said to be Ahlfors-regular if the measure of balls of the same radius are comparable and that the measure scales like an appropriate power of the radius. Formally, we have the following definition.

**Definition 1.3.16.** A metric space  $(X, d)$  is **Ahlfors-regular** of dimension  $\alpha > 0$  if there exists a Borel measure  $\mu$  on  $X$  and a constant  $C \geq 1$  such that for all  $x \in X$  and all  $r \in (0, |X|]$  we have

$$C^{-1}r^\alpha \leq \mu(\overline{B}(x, r)) \leq Cr^\alpha$$

In this case, the constant  $\alpha$  is the Hausdorff dimension of  $X$ , and  $\mu$  is comparable to the  $\alpha$ -dimensional Hausdorff measure, i.e., there exists  $K \geq 1$  such that  $K^{-1}\mu(E) \leq \mathcal{H}^\alpha(E) \leq K\mu(E)$  for all Borel sets  $E \subseteq X$ .

The examples we are considering, and more generally all self-similar subsets of Euclidean space that are generated by an iterated function system that satisfy the open set condition (1.2.1) are Ahlfors-regular, see Theorem 4.14 in [Mat95] or Theorem 8.3.2 in [MT10] for a formal statement. The result originated in a paper by Hutchinson [Hut81]. A frequently useful variant of conformal dimension is the following, introduced by Bourdon and Pajot in [BP03].

**Definition 1.3.17.** Let  $X$  be an Ahlfors-regular metric space. Then the **Ahlfors-regular conformal dimension** is the infimum of the Hausdorff dimensions of quasisymmetrically equivalent Ahlfors-regular metric spaces  $Y$ . We will denote it by  $\dim_{AR} X$ .

The assumption of Ahlfors-regularity on  $X$  is to make sure that  $X$  is quasisymmetrically equivalent to at least one Ahlfors-regular metric space. Every uniformly perfect complete doubling space is quasisymmetrically equivalent to an Ahlfors-regular space [Hei01, Ch. 14].

For an Ahlfors-regular metric space  $X$ , we can extend (1.3.3) to

$$\dim_T X \leq \dim_C X \leq \dim_{AR} X \leq \dim_H X \tag{1.3.4}$$

In general, each one of these inequalities can be strict. We finally can state the conjecture for which we will provide numerical support.

**Conjecture 1.3.18.** Let  $S$  be the Sierpiński carpet, then

$$1.70 < \dim_{AR} S < 1.80.$$

A more complete background regarding conformal dimension, including an extensive bibliography is given in the book by Mackay and Tyson [MT10].

A related notion, the spectral dimension,  $\dim_S$ , has been studied on the Sierpiński carpet, for example, see [BB90] and [KY92]. A numerical value was found by calculations of conductivities of approximations to the carpet in [BBS90], they showed that  $\dim_S S \approx 1.80525$ . In this case the spectral dimension provides an upper bound for the conformal dimension, i.e.  $\dim_C S < \dim_S S \approx 1.80525$ . The numerical approach is entirely different than what we will develop so we will not spend any additional time on the notion.

#### 1.4 Graph Approximations and Modulus

In order to study conformal dimensions explicitly, discretization is a powerful tool, especially for self-similar metric spaces that are already presented as limits of discrete approximations. The key to our approach is that the Ahlfors-regular conformal dimension of a compact metric space is the critical exponent of a sequence of moduli on graph approximations, see Theorem 1.4.13 for a formal statement. This result is proved by Piaggio in [Pia14], and a similar result is used in [BK13], referring to an upcoming paper [KK]. In the following chapters we will adapt an algorithm by Schramm [Sch93] to compute extremal lengths, the reciprocal of the moduli, on the graph approximations.

In the following,  $(X, d)$  will be a compact Ahlfors-regular metric space. In order to apply the result by Piaggio we will need constants  $K \geq 1$ ,  $a > 1$ ,  $\lambda \geq 3$ . For every  $n \geq 1$ , let  $\mathcal{S}_n$  be a finite covering of  $X$  such that for all  $U \in \mathcal{S}_n$  there exists  $x_U \in X$  with

$$B(x_U, K^{-1}r_n) \subseteq U \subseteq B(x_U, Kr_n)$$

where  $r_n = a^{-n}$ . We also require that the balls  $B(x_U, K^{-1}r_n)$  are mutually disjoint for every fixed  $n$ . To this sequence of coverings we associate a sequence of graphs  $G_n^c = (V_n^c, E_n^c)$  as follows. The vertices  $V_n^c$  are the elements  $U \in \mathcal{S}_n$ , and two distinct vertices  $U, U' \in \mathcal{S}_n$  are connected by an edge iff  $B(x_U, \lambda Kr_n) \cap B(x_{U'}, \lambda Kr_n) \neq \emptyset$ . Any such sequence of graphs  $\{G_n^c\}$  is a **covering graph approximation** of  $(X, d)$ .

We adopt two notational conventions. First, a non-negative function  $m : V \rightarrow [0, \infty)$  will be called a (discrete) **metric**. For a fixed  $p \geq 0$ , we define the  $p$ -norm  $\|m\|$  of a metric  $m : V \rightarrow [0, \infty)$  by

$$\|m\|_p = \left( \sum_{v \in V} m(v)^p \right)^{1/p}.$$

In the following we will be considering a fixed  $p$  and will write  $\|\cdot\|$  in place of  $\|\cdot\|_p$ .

We will be interested in a certain 'length' of the set of paths connecting the 'top' to the 'bottom' in a finite graph.

**Definition 1.4.1.** Let  $G(V, E)$  be a finite graph. A **path** is a sequence of vertices  $(v_0, v_1, v_2, \dots, v_n)$  with  $v_j \in V$  for  $0 \leq j \leq n$  and  $(v_{j-1}, v_j) \in E$  for  $1 \leq j \leq n$ .

**Definition 1.4.2.** Let  $G = (V, E)$  be a finite graph, let  $\Gamma$  be a family of subsets of  $V$ , and let  $p \geq 0$  be a constant. For a metric  $m : V \rightarrow [0, \infty)$ , we define the  **$m$ -length**

of  $\Gamma$  by

$$l_m(\Gamma) := \inf \left\{ \sum_{v \in \gamma} m(v) : \gamma \in \Gamma \right\}$$

and the  **$p$ -extremal length** of  $\Gamma$  as

$$L_p(\Gamma) := \sup \left\{ \frac{l_m(\Gamma)^p}{\|m\|^p} : \|m\| > 0 \right\}$$

Although we will typically take  $\Gamma$  to be a set of paths in the graph, and will do so shortly, there is no reason that it must be.

At this point it is worth noting that the extremal length is scaling invariant. Specifically, for  $c > 0$ ,  $l_{cm}(\Gamma)^p = c^p l_m(\Gamma)^p$ , and  $\|cm\|^p = c^p \|m\|^p$ , so that  $l_{cm}(\Gamma)^p / \|cm\|^p = l_m(\Gamma)^p / \|m\|^p$ . Since the scaling factor has no impact on the ratio, we can scale each metric so that the  $m$ -length of  $\Gamma$  is of a prescribed value without altering the supremum  $L_p(\Gamma)$ . With this in mind, we formulate an alternative definition.

**Definition 1.4.3.** Let  $G = (V, E)$  be a finite graph, let  $\Gamma$  be a family of subsets of  $V$ , and let  $p \geq 0$  be a constant. For a metric  $m : V \rightarrow [0, \infty)$ , the  **$p$ -extremal length** of  $\Gamma$  is defined as

$$L_p(\Gamma) := \sup \left\{ \frac{1}{\|m\|^p} : l_m(\Gamma) = 1 \right\}.$$

A closely related idea that will be useful for the remainder of the discussion is the  $p$ -modulus.

**Definition 1.4.4.** Let  $G = (V, E)$  be a finite graph, let  $\Gamma$  be a family of subsets of  $V$ , and let  $p \geq 0$  be a constant. A metric  $m : V \rightarrow [0, \infty)$  is **admissible** (for  $\Gamma$ ) if  $\sum_{v \in \gamma} m(v) \geq 1$  for all  $\gamma \in \Gamma$ . The  $p$ -modulus of  $\Gamma$  is defined as

$$\text{Mod}_p(\Gamma) := \inf \{ \|m\|^p : m \text{ admissible.} \}$$

As is the case in the classical conformal modulus setting, for a given curve family, the  $p$ -extremal length is simply the reciprocal of the  $p$ -modulus, which is clear from the previous two definitions.

**Lemma 1.4.5.** *Let  $G = (V, E)$  be a finite graph, let  $\Gamma$  be a family of subsets of  $V$ , and let  $p \geq 0$  be a constant, then*

$$\text{Mod}_p \Gamma = \frac{1}{L_p(\Gamma)}.$$

**Definition 1.4.6.** Let  $G = (V, E)$  be a finite graph and let  $A, B$  be non-empty subsets of  $V$ . Then  $\Gamma(A, B)$  is defined as the set of all paths in  $G$  which connect  $A$  to  $B$ , i.e., having initial vertex in  $A$  and terminal vertex in  $B$ . Additionally, the  **$p$ -extremal length** of this family of paths is  $L_p(A, B) := L_p(\Gamma(A, B))$ , and its  **$p$ -modulus** is  $\text{Mod}_p(A, B) := \text{Mod}_p(\Gamma(A, B))$ .

**Definition 1.4.7.** Let  $\Gamma$  be a family of curves on the compact metric space  $(X, d)$ , and let  $\{G_n^c\}$  be a covering graph approximation with associated sequence of coverings  $\{\mathcal{S}_n\}$ . Then for  $p \geq 0$  the  **$G_n^c$ -combinatorial  $p$ -modulus** of  $\Gamma_n^c = \pi_n(\Gamma)$  is  $\text{Mod}_p(\Gamma_n^c)$ , where  $\gamma \in \Gamma$  projects to  $\pi_n(\gamma) \in \Gamma_n^c$  containing a vertex  $U \in \mathcal{S}_n$  iff  $\gamma \cap U \neq \emptyset$ .

In [Pia], Piaggio characterized the Ahlfors-regular conformal dimension of general Ahlfors-regular compact metric spaces, using critical exponents for graph approximations. The situation simplifies a little for 'approximately self-similar' metric spaces, see [Pia, Section 3.6] and [BK13].

**Definition 1.4.8.** A compact metric space  $(X, d)$  is **approximately self-similar** if there exists  $c > 0$  and  $L \geq 1$  such that for any  $r \in (0, |X|)$  and any  $x \in X$  there exists an open set  $U \subseteq X$  with  $|U| \geq c$  and a  $L$ -bi-Lipschitz map  $\phi : (B(x, r), r^{-1}d) \rightarrow (U, d)$ .

This definition implies that balls at any scale have rescaled bi-Lipschitz images at a uniformly large scale. Any limit set of an Iterated Function System generated by similarities satisfying the open set condition (1.2.1) is approximately self-similar. This follows from a result of Hutchinson [Hut81, Theorem 5.3 (1)].

**Definition 1.4.9.** Let  $(X, d)$  be a compact metric space with a sequence of covering graph approximations  $\{G_n^c\}$ . For  $\delta > 0$  define  $\Gamma(\delta)$  as the family of all curves  $\gamma \subseteq X$  with  $|\gamma| \geq \delta$ . Furthermore,  $\Gamma_n^c(\delta) := \pi_n(\Gamma(\delta))$  is the corresponding sequence of families of paths in the graph approximations, and  $M_{n,p}(\delta) := \text{Mod}_p(\Gamma_n^c(\delta))$  is the sequence of their combinatorial  $p$ -moduli.

**Definition 1.4.10.** Suppose  $(X, d)$  is a compact connected metric space. For  $x, y \in X$  define

$$\delta(x, y) := \inf \{|J| : J \text{ is compact connected and } x, y \in J\}.$$

For  $r > 0$  let

$$h(r) := \sup \{\delta(x, y) : d(x, y) \leq r\}.$$

We say that  $X$  is **locally connected** if  $h(r) \rightarrow 0$  as  $r \rightarrow 0$ . We say that  $X$  is **linearly connected** if there exists a constant  $K \geq 1$  such that  $h(r) \leq Kr$  for all  $0 < r \leq |X|$ .

We note that in the case  $X$  is linearly connected, the distances  $\delta$  and  $d$  are bi-Lipschitz equivalent; in particular,  $d \leq \delta \leq Kd$ .

The following definition and theorem were given in [BK13, Corollary 3.7] and will be central to our argument.

**Definition 1.4.11.** The **critical exponent** associated to the curve family  $\Gamma(\delta)$  is defined as

$$Q_\delta := \inf \left\{ p \geq 1 : \lim_{n \rightarrow \infty} M_{n,p}(\delta) = 0 \right\}$$

**Theorem 1.4.12** (Bourdon and Kleiner). *For  $\delta > 0$  we have the following.*

- (1) *For  $p > Q_\delta$  one has  $\lim_{n \rightarrow \infty} M_{n,p}(\delta) = 0$ .*
- (2) *For  $1 \leq p \leq Q_\delta$  the sequence  $\{M_{n,p}(\delta)\}_{n \geq 0}$  admits a positive lower bound.*
- (3) *If  $(X, d)$  is linearly connected, then for  $1 \leq p < Q_\delta$  the sequence  $\{M_{n,p}(\delta)\}_n$  is unbounded.*

If an approximately self-similar metric space is connected and locally connected, then it is linearly connected [Pia11, Chapter 2]. Since the Sierpiński carpet is connected and locally connected, it is linearly connected and (3) will apply.

Furthermore, we have the following central result, see [Pia, Corollary 3.14].

**Theorem 1.4.13** (Piaggio). *Let  $(X, d)$  be an approximately self-similar compact metric space with a covering graph approximation  $\{G_n^e\}$ . Assume furthermore that  $X$  is connected and locally connected. Then there exists  $\delta_0 > 0$  such that  $\dim_{AR} X = Q_\delta$  for all  $\delta \in (0, \delta_0)$ .*

We are interested in applying these theorems to the Sierpiński carpet. We do so now.

### 1.5 Graph Approximation of the Sierpiński Carpet

Let  $S_0 = [0, 1]^2$  be the unit square. Consider subdividing  $S_0$  into nine congruent subsquares of side length  $\frac{1}{3}$  with disjoint interiors. Let  $\mathcal{SC}_1$  be the set of eight subsquares remaining after removing the central subsquare, and let  $S_1 = \bigcup\{s : s \in \mathcal{SC}_1\}$ . Repeating the process, subdivide each element of  $\mathcal{SC}_1$  into nine congruent subsquares of side length  $\frac{1}{9}$  with disjoint interiors. Let  $\mathcal{SC}_2$  be the set of 64 subsquares remaining after removing the central subsquare from each element of  $\mathcal{SC}_1$ , and let

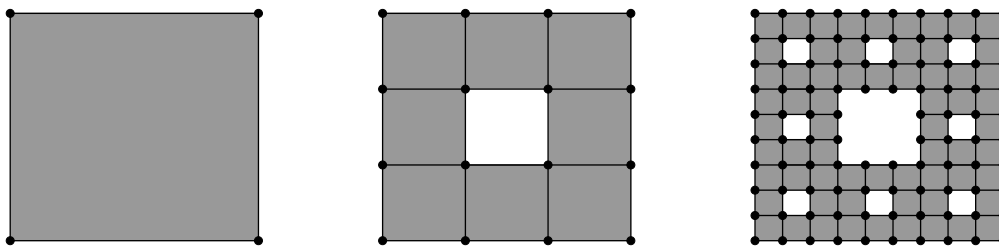


Figure 1.7:  $S_0, S_1$ , and  $S_2$  in gray.  $E_0, E_1$ , and  $E_2$  represented by black line segments.  $V_0, V_1$ , and  $V_2$  represented by points.

$S_2 = \bigcup \{s : s \in \mathcal{SC}_2\}$ . Continuing in this manner, we construct a decreasing sequence of compact sets  $\{S_n\}_{n \geq 0}$  and obtain the standard Sierpiński carpet

$$S := \bigcap_{n \geq 0} S_n.$$

Let  $\mathcal{E}_0$  be the boundary of  $S_0$ , considered as four separate line segments. Specifically, the top  $[0, 1] \times \{1\}$ , the bottom  $[0, 1] \times \{0\}$ , the left  $\{0\} \times [0, 1]$ , and the right  $\{1\} \times [0, 1]$ . Let  $\mathcal{E}_1$  be the set of 24 unique line segments that form the boundaries of the subsquares in  $\mathcal{SC}_1$ . In general, for each  $n \geq 0$ , let  $\mathcal{E}_n$  be the unique set of line segments that form the boundaries of the subsquares in  $\mathcal{SC}_n$ .

Let  $\mathcal{V}_0$  be the four points of intersection of the line segments in  $\mathcal{E}_0$ . Let  $\mathcal{V}_1$  be the 16 unique points of intersection of the line segments in  $\mathcal{E}_1$ . In general, for  $n \geq 0$ , let  $\mathcal{V}_n$  be the unique points of intersection of the line segments in  $\mathcal{E}_n$ .

For each  $n \geq 0$ , the sets  $\mathcal{E}_n$  and  $\mathcal{V}_n$  form a planar graph. To each we associate a combinatorial finite connected graph approximation of the Sierpiński carpet  $A_n = (V_n, E_n)$  in the obvious way. We will refer to the graph approximations  $A_n$  as the **standard graph approximations** and to the sets  $V_n$  and  $E_n$  as the sets of **vertices** and **edges** respectively. Combinatorially, the scaling is not relevant, so we will typically visualize the graph approximations with uniform edge lengths, regardless of

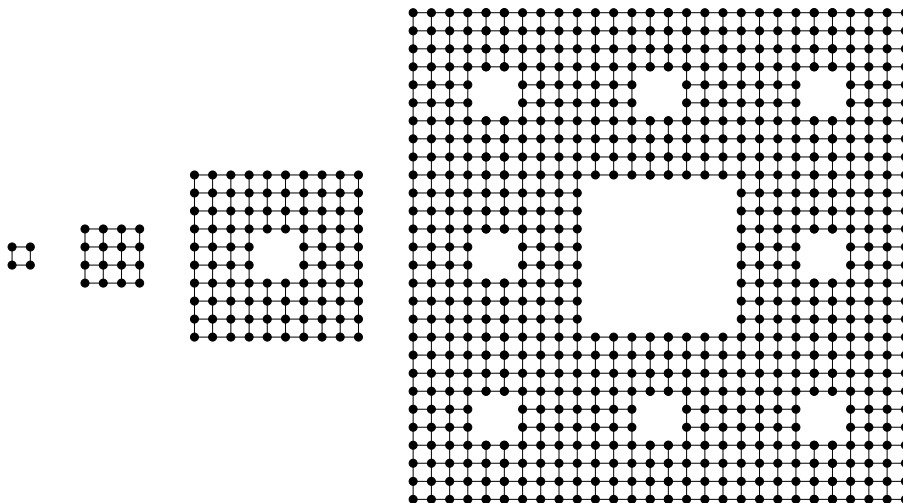


Figure 1.8: Graph approximations  $A_0, A_1, A_2$ , and  $A_3$ .

scale; see, for example, Figure 1.8.

Of interest to us will be the subsets of vertices corresponding to the four sides. Specifically, for each  $n \geq 0$  we let the **top** be the subset  $T_n \subset V_n$  composed of vertices associated with points in  $\mathcal{V}_n$  of the form  $(x, 1)$ . Similarly, the **bottom** is the subset  $B_n \subset V_n$  composed of vertices associated with points of the form  $(x, 0)$ . The **left** subset  $L_n \subset V_n$  is composed of vertices associated with points of the form  $(0, y)$ . The **right** subset  $R_n \subset V_n$  is composed of vertices with points of the form  $(1, y)$ .

For the covering graph approximation at the  $n$ -th stage we choose the covering by balls  $U$  of radius  $r_n = 3^{-n}$  centered at vertices  $x_U$  of the squares from the construction of the Sierpiński carpet  $\mathcal{SC}_n$  that correspond to  $V_n$ . Since the balls of radius  $r_n$  centered at the vertices of a square of side length  $r_n$  cover the square,  $\mathcal{S}_n$  is a covering of  $S_n$ , and thus a covering of the carpet  $S \subset S_n$ . We then choose  $K = 2$ ,  $a = 3$ ,  $\lambda = 3$ , and it is easy to check that all the conditions of a covering graph approximation are satisfied. Let  $G_n^c = (V_n^c, E_n^c)$  be the associated covering graph. The vertices of  $G_n^c$  and  $A_n$  are canonically identified, since they both correspond to vertices of squares in  $S_n$ .

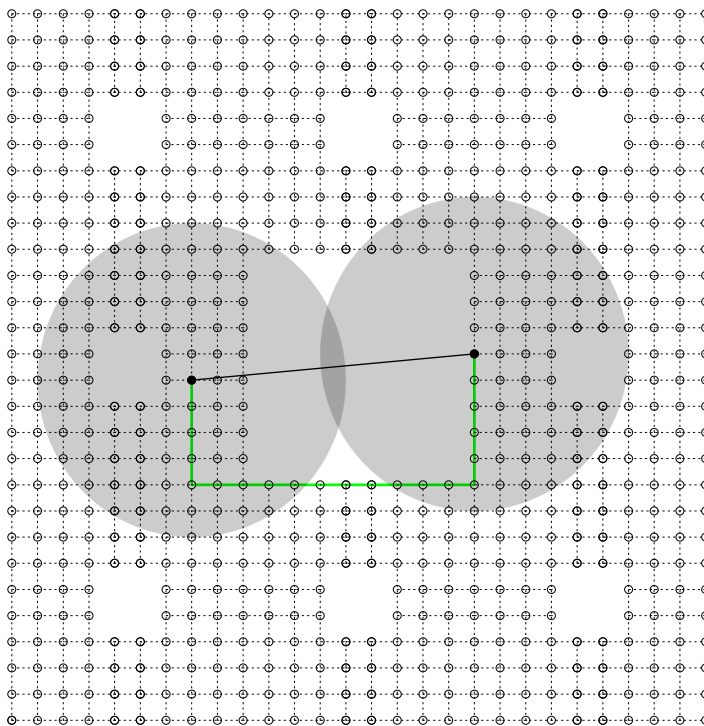


Figure 1.9: An edge (solid black line) in the covering graph  $G_3^c$  connecting vertices with graph distance 1 while the corresponding graph distance in the standard graph approximation has graph distance 20 shown by the green edges.

Now  $G_n^c$  has more edges for all  $n \geq 1$  than  $A_n$ , but the following lemma shows that they are equivalent up to a uniformly bi-Lipschitz family of maps. In the following Lemma, the distances  $d_g(x, y)$  are graph distances, i.e., the minimum number of edges connecting  $x$  to  $y$ . Figure 1.9 is helpful to have in mind while reading the proof.

**Lemma 1.5.1.** *Let  $f_n : V_n^c \rightarrow V_n$  be the canonical map between the vertices of  $G_n^c$  and  $A_n$ . Then  $f_n$  is bi-Lipschitz with respect to graph distances, where the bi-Lipschitz constant can be chosen independent of  $n$ . More precisely,*

$$d_g(u, v) \leq d_g(f_n(u), f_n(v)) \leq 24d_g(u, v)$$

for all  $u, v \in V_n^c$ .



To reach the opposite side of a 2 by 2 void, the detour,  $D$ , is at most two edges since the shorter of the two possible routes is at most one edge in each direction, see Figure 1.10. The red edges are the detour, the blue edges are accounted for by  $H$  and  $V$ . Similarly, to reach the opposite side of a 8 by 8 void, the detour,  $D$ , is at most eight edges. Again, the shorter of the two is at most four in each direction. Since  $H, V \leq 12$  at most one detour is required.

Since we have  $d_g(f_n(u), f_n(v)) = H + V + D$  and  $H + V + D \leq 16 + 8$  we conclude  $d_g(f_n(u), f_n(v)) \leq 24d_g(u, v)$ .  $\square$

We remark that a stronger upper bound of  $d_g(f_n(u), f_n(v)) \leq 20d_g(u, v)$  is true. Since the particular value of the constant does not change the outcome of the upcoming argument, we leave the details as an exercise for the interested reader.

**Lemma 1.5.2.** *Let  $G_k = (V_k, E_k)$  be graphs for  $k = 1, 2$ , and let  $f : G_1 \rightarrow G_2$  be  $L$ -bi-Lipschitz in the graph metric. Let  $A_1$  and  $B_1$  be non-empty subsets of  $V_1$ , and let  $A_2 = f(A_1)$ ,  $B_2 = f(B_1)$ . Then*

$$L^{-p} \text{Mod}_p(A_2, B_2) \leq \text{Mod}_p(A_1, B_1) \leq L^p \text{Mod}_p(A_2, B_2)$$

*Proof.* Let  $\Gamma_1 := \Gamma(A_1, B_1)$  and  $\Gamma_2 := \Gamma(A_2, B_2)$ , and let  $\rho_2$  be an admissible metric for  $\Gamma_2$ . Define  $\rho_1(v) := L\rho_2(f(v))$ . Then  $\rho_1$  is admissible for  $\Gamma_1$ , and

$$\sum_{v \in V_1} \rho_1^p(v) = L^p \sum_{v \in V_2} \rho_2^p(v)$$

Taking the infimum over all admissible metrics  $\rho_2$  gives

$$\text{Mod}_p(A_1, B_1) \leq L^p \text{Mod}_p(A_2, B_2)$$

The reverse inequality follows by applying the same argument to  $f^{-1}$ .  $\square$

**Corollary 1.5.3.** *Let  $G_n^c = (V_n^c, E_n^c)$  and  $A_n = (V_n, E_n)$  be the covering and standard graph approximations to the Sierpiński carpet. Let  $\Gamma_n^c$  and  $\Gamma_n$  be the families of path connecting the top and bottom edges of  $G_n^c$  and  $A_n$ , respectively. Then*

$$1 \leq \frac{\text{Mod}_p(\Gamma_n^c)}{\text{Mod}_p(\Gamma_n)} \leq 24^p$$

*Proof.* This follows directly from the last two lemmas. Also note that the moduli can not be zero, so the quotient is well-defined.  $\square$

In order to apply Theorem 1.4.12 to our situation, we will show the critical exponent is the same for  $\Gamma(\delta)$  as it is for  $\Gamma(T, B)$ , where  $T$  and  $B$  are the top and bottom of the carpet. The fact that the critical exponent for the standard and covering graph approximations are the same follows from the uniform bi-Lipschitz equivalence between these two graph approximations, proved in Corollary 1.5.3.

**Theorem 1.5.4.** *Let  $S$  be the Sierpiński carpet and  $\{G_n^c\}$  be the covering approximation. Let  $\delta \in (0, 1)$  and  $p \geq 1$ . Then there exist constants  $C = C(\delta)$  and  $N = N(\delta)$  such that*

$$M_{n,p}(T, B) \leq M_{n,p}(\delta) \quad \text{and} \quad M_{N+n,p}(\delta) \leq CM_{n,p}(T, B)$$

for all  $n$ , where  $T$  and  $B$  are the top and bottom of the carpet, and  $M_{n,p}(T, B) = \text{Mod}_{n,p}(\Gamma^c(T, B))$  is the  $G_n^c$ -combinatorial  $p$ -modulus of the family of curves connecting  $T$  to  $B$ .

*Proof.* The first inequality is straight-forward. If  $m$  is admissible on  $G_n^c$  for  $\Gamma_n(\delta)$ , then  $m$  is also admissible for  $\Gamma_n^c(T, B)$ , since every curve  $\gamma$  connecting  $T$  to  $B$  has

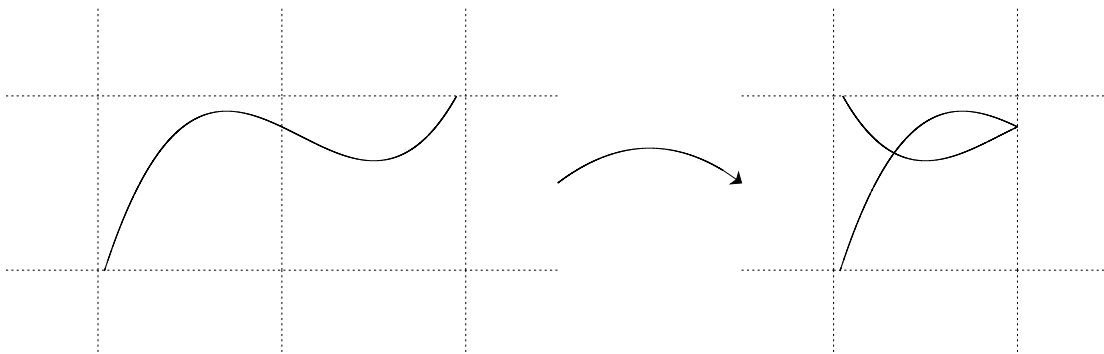


Figure 1.11: A curve  $\gamma$  in  $G_{N+n}^c$  is reflected so that a part of it is fully contained in a square at the  $N$ -th stage and connects the top and bottom.

diameter  $|\gamma| \geq 1 > \delta$ .

In order to prove the second inequality, assume that  $m$  is admissible on  $G_n^c$  for  $\Gamma_n^c(\delta)$ . We would like  $m$  to be symmetric under rotations and reflections of the square, however there is no reason to suspect that it is. To assure the symmetry, define  $\hat{m}$  to be the sum of  $m$  composed with the eight elements of the dihedral group of order 8, i.e. the symmetries of the square. By construction  $\hat{m}$  is then admissible for the curve family connecting the left boundary to the right boundary in addition to being admissible for the curve family connecting the top to the bottom.

Now choose  $N \in \mathbb{N}$  large enough so that  $3^{-N} \cdot 2\sqrt{2} < \delta$  and let  $\hat{m}_N$  on  $G_{N+n}^c$  be the metric obtained by summing the images of  $\hat{m}$  under the  $8^N$  contractions at the  $N$ -th stage of the construction of the Sierpiński carpet. By construction  $\hat{m}_N$  is admissible for the family of curves that connect opposing sides of the  $N$ -th stage squares of the construction in  $G_{N+n}^c$ . By our choice of  $N$  any curve  $\gamma$  of diameter  $|\gamma| \geq \delta$  must cross two adjacent vertical or horizontal lines of the grid at the  $N$ -th stage of the construction. Assume that it crosses two adjacent horizontal lines, see Figure 1.11. By reflecting  $\gamma$  across vertical lines of the  $N$ -th stage of the construction we can assume that a part of  $\gamma$  is fully contained in a square at the  $N$ -th construction

stage and connects the top to the bottom. By construction  $\hat{m}_N$  is symmetric with respect to these reflections. This shows that  $\hat{m}_N$  is admissible for  $\Gamma_{N+n}^c(\delta)$ . Applying Minkowski's inequality we have

$$M_{N+n,p}(\delta) \leq 8^N \sum_{v \in V_n} \hat{m}(v)^p \leq 8^N 8^p \sum_{v \in V_n} m(v)^p.$$

Taking the infimum over admissible metrics we get

$$M_{N+n,p}(\delta) \leq 8^{N+p} M_{n,p}(T, B).$$

If  $\gamma$  crosses two adjacent vertical lines of the  $N$ -th construction stage the argument is entirely similar. □

**Corollary 1.5.5.** *The critical exponents for  $\Gamma_n(T, B)$  and  $\Gamma_n(\delta)$  in the covering and standard graph approximations are all the same.*

*Proof.* Since the curve families are non-empty, this follows directly from the preceding theorem, Corollary 1.5.3, and the definition of the critical exponent in Definition 1.4.11. □

## ALGORITHM FOR EXTREMAL LENGTH

In this chapter we develop an algorithm to compute the extremal length for graphs, the standard graph approximations of the Sierpiński carpet in particular. The algorithm in Section 2.3 is based on a similar algorithm developed by Schramm [Sch93].

### 2.1 Combinatorics of the Standard Graph Approximations

We focus our attention on the standard graph approximations of the Sierpiński carpet  $A_n = (V_n, E_n)$  as defined in Section 1.5. We recall the subsets of  $V_n$  that correspond to the four sides, the top  $T_n$ , the bottom  $B_n$ , the left  $L_n$  and the right  $R_n$ . Beyond the sides, we will also be interested in subsets of vertices that separate a graph in a particular way. We will need a bit more machinery to implement that idea. Recall that a path is a sequence of vertices, see Definition 1.4.1, and that  $\Gamma(A, B)$  is the set of paths from  $A$  to  $B$ , see Definition 1.4.6.

**Definition 2.1.1.** Let  $G = (V, E)$  be a finite graph and let  $A, B$  be non-empty subsets of  $V$ . A subset  $D \subset V$  is said to **separate**  $A$  from  $B$  if  $\gamma \cap D \neq \emptyset$  for every  $\gamma \in \Gamma(A, B)$ . We will say a separating set is **minimal** if  $\#D = \min\{\#D' : D' \text{ separates } A \text{ from } B\}$ . Here, and throughout this chapter, we use the notation  $\#U$  to represent the cardinality of a set  $U$ .

It will be convenient to discuss the graph approximation  $A_{n+1}$  in terms of the eight embedded copies of  $A_n$  that are subsets of it. Notationally we write

$$A_{n+1} = A_{n,\nwarrow} \cup A_{n,\uparrow} \cup A_{n,\nearrow} \cup A_{n,\leftarrow} \cup A_{n,\rightarrow} \cup A_{n,\swarrow} \cup A_{n,\downarrow} \cup A_{n,\searrow}. \quad (2.1.1)$$

The subsets are clearly not disjoint. For example, the bottom subset of  $A_{n,\nwarrow}$  coincides with the top subset of  $A_{n,\leftarrow}$  and the right subset of  $A_{n,\nwarrow}$  coincides with the

$A_{n,\nwarrow}$	$A_{n,\uparrow}$	$A_{n,\nearrow}$
$A_{n,\leftarrow}$		$A_{n,\rightarrow}$
$A_{n,\swarrow}$	$A_{n,\downarrow}$	$A_{n,\searrow}$

Figure 2.1: Embeddings of  $A_n$  into  $A_{n+1}$ 

left subset of  $A_{n,\uparrow}$ , i.e.  $B_{n,\nwarrow} = T_{n,\leftarrow}$  and  $R_{n,\nwarrow} = L_{n,\uparrow}$ . See Figure 2.1.

**Lemma 2.1.2.** *For the graph approximation  $A_n = (V_n, E_n)$ , we have*

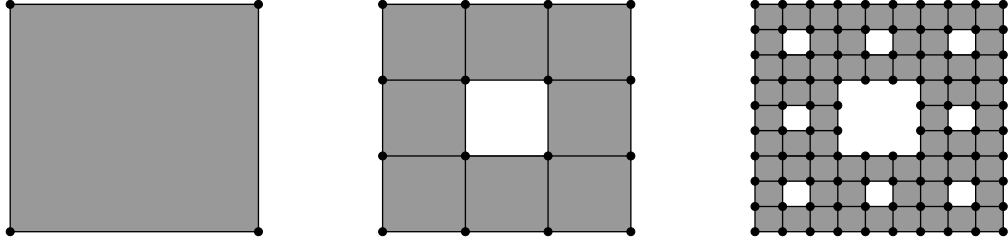
$$\#L_n = \#R_n = \#T_n = \#B_n = 3^n + 1 \quad \text{for } n \geq 0 \quad (2.1.2)$$

$$\#V_0 = 4, \#V_1 = 16, \text{ and}$$

$$\#V_n = (3^n + 1)^2 - \sum_{k=0}^{n-2} 8^k (3^{n-1-k} - 1)^2 \quad \text{for } n \geq 2 \quad (2.1.3)$$

*Proof.* By symmetry  $\#L_n = \#R_n = \#T_n = \#B_n$ , so we consider just  $L_n$  and proceed by induction.  $L_0$  contains the vertices corresponding to the points  $(0, 0)$  and  $(0, 1)$  in the planar graph, so  $\#L_0 = 2 = 3^0 + 1$ . Now, assume  $\#L_n = 3^n + 1$ . Since  $L_{n+1} = L_{n,\nwarrow} \cup L_{n,\leftarrow} \cup L_{n,\swarrow}$  with two vertices coinciding,  $\#L_{n+1} = 3(3^n + 1) - 2 = 3^{n+1} + 1$  as required.

To show the second set of equations, we note that the number of vertices in  $V_0$  and  $V_1$  is clear; for clarity see Figure 2.2. For the remaining cases, we argue by induction.  $\#V_2 = 96 = (3^2 + 1)^2 - 8^0 (3^1 - 1)^2$  since  $A_2$  consists of a ten by ten grid of vertices with the four central vertices removed. Now, assume  $\#V_n = (3^n + 1)^2 - \sum_{k=0}^{n-2} 8^k (3^{n-1-k} - 1)^2$ .  $A_{n+1}$  consists of eight embedded copies of  $A_n$  with eight sides coinciding. For example, the bottom subset of  $A_{n,\nwarrow}$  coincides with the

Figure 2.2:  $A_0, A_1,$  and  $A_2$ .

top subset of  $A_{n,\leftarrow}$ . There are seven other coinciding pairs. Since all side are of the same size, we use  $T_n$  in the following to represent each side regardless of the actual coincident side. A routine calculation using (2.1.2) then shows

$$\begin{aligned}
\#V_{n+1} &= 8\#V_n - 8\#T_n \\
&= 8(\#V_n - \#T_n) \\
&= 8\left((3^n + 1)^2 - \sum_{k=0}^{n-2} 8^k (3^{n-1-k} - 1)^2 - (3^n + 1)\right) \\
&= 8 \cdot 3^{2n} + 8 \cdot 3^n - \sum_{k=0}^{n-2} 8^{k+1} (3^{n-1-k} - 1)^2 \\
&= (9 \cdot 3^{2n} + 6 \cdot 3^n + 1) - (3^{2n} - 2 \cdot 3^n + 1) - \sum_{k=0}^{n-2} 8^{k+1} (3^{n-1-k} - 1)^2 \\
&= (3^{2n+2} + 2 \cdot 3^{n+1} + 1) - 8^0 (3^n - 1)^2 - \sum_{j=1}^{(n+1)-2} 8^j (3^{(n+1)-1-j} - 1)^2 \\
&= (3^{n+1} + 1)^2 - \sum_{j=0}^{(n+1)-2} 8^j (3^{(n+1)-1-j} - 1)^2.
\end{aligned}$$

(2.1.3) then follows by induction. □

**Lemma 2.1.3.** *For the graph approximation  $A_n$ , let  $D_n \subset A_n$  be a minimal set separating  $T_n$  from  $B_n$ , then*

$$\#D_n = 2^{n+1}. \tag{2.1.4}$$

We will call such a set a **minimal horizontal separating set** since it separates the top and the bottom of the graph approximation.

*Proof.* The argument will proceed by induction in two parts. First, that there are  $2^{n+1}$  vertical paths in  $A_n$ , and hence  $\#D_n \geq 2^{n+1}$  since at least one vertex from each vertical path must be in  $D_n$ . Second, we will show there exists a disconnecting set  $D'_n$  with  $\#D'_n = 2^{n+1}$ , and hence  $D'_n$  is a minimal horizontal separating set. Before we begin, define a vertical path as a set of vertices with initial vertex in the top, terminal vertex in the bottom, and all vertices corresponding to points with the same  $x$ -coordinate. Geometrically, a vertical path corresponds to a vertical segment from the top to the bottom.

For  $A_0$ , it is clear that there are two vertical paths, specifically,  $R_0$  and  $L_0$ , the right and left subsets, respectively. Since any path from the top to the bottom must contain one of the two, we also see that choosing a set  $D'_0$  composed of one vertex from  $R_0$  and one vertex from  $L_0$  is a separating set. Hence,  $D'_0$  is a minimal horizontal separating set with  $\#D'_0 = 2$ .

Now, assume that the graph approximation  $A_n$  has  $2^{n+1}$  vertical paths and a minimal horizontal separating set  $D_n$  with  $\#D_n = 2^{n+1}$ . Since  $A_{n+1}$  has eight embedded copies of  $A_n$ , it is a simple matter of concatenating geometrically corresponding vertical paths in  $A_{n,\swarrow}, A_{n,\leftarrow},$  and  $A_{n,\searrow}$  to create  $2^{n+1}$  vertical paths in  $A_{n+1}$ . We note that the terminal vertex of a vertical path in  $A_{n,\swarrow}$  and the initial vertex of the corresponding vertical path in  $A_{n,\leftarrow}$  coincide. In this case, and other cases of coincident vertices, the concatenation is understood to include that vertex only once. Similarly, we concatenate the geometrically corresponding vertical paths in  $A_{n,\nearrow}, A_{n,\rightarrow},$  and  $A_{n,\searrow}$  to create  $2^{n+1}$  additional vertical paths in  $A_{n+1}$ . Together we have  $2^{n+2}$  vertical paths in  $A_{n+1}$ , and hence  $\#D_{n+1} \geq 2^{n+2}$ .

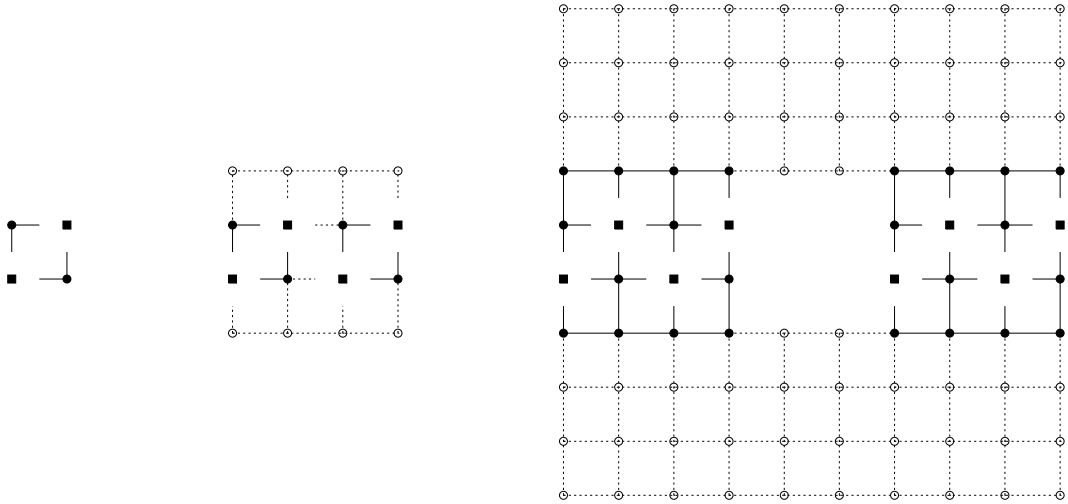


Figure 2.3: Represented by squares, examples of minimal horizontal separating sets  $D_0$ ,  $D_1$ , and  $D_2$ . The embedding of  $D_{0,\leftarrow} \subset A_{0,\leftarrow}$  and  $D_{0,\rightarrow} \subset A_{0,\rightarrow}$  is highlighted in  $A_1$ . Similarly, the embedding of  $D_{1,\leftarrow} \subset A_{1,\leftarrow}$  and  $D_{1,\rightarrow} \subset A_{1,\rightarrow}$  is highlighted in  $A_2$ .

Let  $D_{n,\leftarrow}$  be the assumed minimal horizontal separating set in  $A_{n,\leftarrow}$ , similarly let  $D_{n,\rightarrow}$  be the assumed minimal horizontal separating set in  $A_{n,\rightarrow}$ . Any path from the top to the bottom of  $A_{n+1}$  must either contain a path from the top to the bottom of  $A_{n,\leftarrow}$ , or a path from the top to the bottom of  $A_{n,\rightarrow}$ . Since  $D_{n,\leftarrow}$  separates  $A_{n,\leftarrow}$  and  $D_{n,\rightarrow}$  separates  $A_{n,\rightarrow}$ , letting  $D'_{n+1} = D_{n,\leftarrow} \cup D_{n,\rightarrow}$  generates a horizontal separating set of  $A_{n+1}$ . The sets  $D_{n,\leftarrow}$  and  $D_{n,\rightarrow}$  are disjoint, so we conclude that  $D'_{n+1}$  is a minimal horizontal separating set with  $\#D'_{n+1} = 2^{n+2}$ , as required.

By induction, we see (2.1.4) holds for all  $n \geq 0$ . □

## 2.2 Extremal Length in Graphs

It will be useful to have some additional notation regarding the idea of extremal length before we develop the algorithm. For convenience we combine our earlier definitions of extremal length, Definitions 1.4.2 and 1.4.6, and introduce the normalized

length. As before,  $\Gamma(A, B)$  is the set of all paths from  $A$  to  $B$ , a discrete metric is a function  $m : V \rightarrow [0, \infty)$ , and the norm is taken to be the  $p$ -norm for a fixed  $p > 1$ .

**Definition 2.2.1.** Let  $G = (V, E)$  be a finite graph with  $A, B$  non-empty subsets of  $V$ . For the family of paths  $\Gamma(A, B)$  and a metric  $m : V \rightarrow [0, \infty)$ , the  **$m$ -length** of  $\Gamma(A, B)$  is

$$l_m(A, B) := \inf \left\{ \sum_{v \in \gamma} m(v) : \gamma \in \Gamma(A, B) \right\}$$

and the **normalized length** of  $\Gamma(A, B)$  is defined as

$$\hat{l}_m(A, B) := \frac{(l_m(A, B))^p}{\|m\|^p}.$$

Additionally, we define the  **$p$ -extremal length** as

$$L_p(A, B) := \sup \left\{ \hat{l}_m(A, B) : \|m\| > 0 \right\}.$$

An **extremal metric** is one which achieves this supremum.

A related concept of a dual-length will be useful before we begin discussing the algorithm.

**Definition 2.2.2.** Let  $G = (V, E)$  be a finite graph with  $U$  a non-empty subset of  $V$ . For a metric  $m : V \rightarrow [0, \infty)$  the  **$m$ -dual-length** of  $U$  is

$$l_m^*(U) := \sum_{v \in U} m(v)^{p-1}.$$

If  $A, B$  are non-empty subsets of  $V$  then the  **$m$ -dual-length** of  $A, B$  is defined

$$l_m^*(A, B) := \inf \{ l_m^*(U) : U \subset V, U \text{ separates } A \text{ from } B \}.$$

With the definitions in hand, we state a fundamental result. The following theorem and proof are an adapted and expanded version of a result and proof by Schramm [Sch93, Theorem 9.1].

**Theorem 2.2.3.** *Let  $G = (V, E)$  be a finite graph with  $A, B$  non-empty subsets of  $V$ . Let  $m : V \rightarrow [0, \infty)$  be a metric with  $\|m\| > 0$  and let  $1 < p < \infty$ .*

(1) *An extremal metric  $M$  exists and is unique up to a positive scaling factor.*

(2) *It holds that*

$$l_m(A, B)l_m^*(A, B) \leq \|m\|^p \quad (2.2.1)$$

$$(l_m^*(A, B))^p \leq \frac{\|m\|^{p(p-1)}}{\hat{l}_M(A, B)}, \quad (2.2.2)$$

*with equality holding in both if  $m$  is extremal. Additionally, equality in either implies  $m$  is extremal.*

*Proof.* Let  $C$  be the set of all metrics with  $l_m(A, B) \geq 1$ . Then  $C$  is a non-empty, closed, and convex set. Since  $1 < p < \infty$ , the space of metrics with the  $p$ -norm is strictly convex and finite dimensional; it follows that there exists a unique element  $m_0 \in C$  of minimal norm. Let  $m_1$  be any metric with  $l_{m_1}(A, B) > 0$ . Then  $m_1/l_{m_1}(A, B) \in C$ , and (1) follows from the scaling invariance of  $(l_m(A, B))^p / \|m\|^p$  in the sense that  $l_{cm}(A, B) = cl_m(A, B)$  for any positive scaling factor  $c$ .

For a metric  $m_1 : V \rightarrow [0, \infty)$  we would like a family of separating sets that consist of vertices  $v \in V$  of similar  $m_1$ -distance from  $A$ . Formally, let  $l_{m_1}(A, \{v\})$  be the  $m_1$ -length of the family of paths from  $A$  to the vertex  $v$  and then for each  $t \in \mathbb{R}$  we define  $U_{m_1}(t) = \left\{ v \in V : l_{m_1}(A, \{v\}) - m_1(v) \leq t < l_{m_1}(A, \{v\}) \right\}$ . Note that for each  $t \in [0, l_{m_1}(A, B))$ ,  $U_{m_1}(t)$  separates  $A$  from  $B$ .

To show (2) we let  $m_1, m_2 : V \rightarrow [0, \infty)$  be metrics and proceed as follows.

$$\begin{aligned}
l_{m_1}(A, B)l_{m_2}^*(A, B) &\leq \int_0^{l_{m_1}(A, B)} l_{m_2}^*(U_{m_1}(t)) dt \\
&= \int_0^{l_{m_1}(A, B)} \sum_{v \in U_{m_1}(t)} m_2(v)^{p-1} dt \\
&\leq \sum_{v \in V} \int_{l_{m_1}(A, \{v\}) - m_1(v)}^{l_{m_1}(A, \{v\})} m_2(v)^{p-1} dt \\
&= \sum_{v \in V} m_1(v) m_2(v)^{p-1} \\
&\leq \left( \sum_{v \in V} m_1(v)^p \right)^{1/p} \left( \sum_{v \in V} m_2(v)^p \right)^{(p-1)/p} \\
&= \|m_1\| \|m_2\|^{p-1}
\end{aligned} \tag{2.2.3}$$

The first inequality follows since  $l_{m_2}^*(A, B)$  is an infimum, the second follows from Fubini's Theorem and  $\{v \in V : v \in U_{m_1}(t) \text{ for some } t \in [0, l_{m_1}(A, B)]\} \subseteq V$ , and the third is an application of Hölder's inequality. (2.2.1) follows from (2.2.3) by letting  $m_1 = m_2 = m$ . Letting  $m_1 = M$  (an extremal metric) and  $m_2 = m$ , (2.2.2) follows from (2.2.3) by raising both sides to the  $p$  power and combining terms.

Now assume equality holds in (2.2.1) for  $m$ , i.e.  $l_m(A, B)l_m^*(A, B) = \|m\|^p$ . It follows that

$$(l_m^*(A, B))^p = \frac{\|m\|^{p(p-1)}}{\hat{l}_m(A, B)}.$$

Now making use of  $\hat{l}_m(A, B) \leq \hat{l}_M(A, B)$  and (2.2.2) we have

$$(l_m^*(A, B))^p = \frac{\|m\|^{p(p-1)}}{\hat{l}_m(A, B)} \geq \frac{\|m\|^{p(p-1)}}{\hat{l}_M(A, B)} \geq (l_m^*(A, B))^p$$

which implies  $\hat{l}_m(A, B) = \hat{l}_M(A, B)$ , allowing us to conclude that  $m$  is extremal.

If equality holds in (2.2.2) for  $m$ , then equality also holds in (2.2.3) with  $m_1 = m$

and  $m_2 = M$ . In particular, equality holds in Hölder so  $m$  is a scalar multiple of  $M$  and hence extremal.

To show equality in the case of an extremal metric, let  $M$  be an extremal metric. Let  $U \subset V$  separate  $A$  from  $B$  with  $l_M^*(U) = l_M^*(A, B)$ . Since the graph is finite the infimum is achieved. For  $t \geq 0$  define  $M_t : V \rightarrow [0, \infty)$  as  $M_t(v) = M(v) + t$  for  $v \in U$  and  $M_t(v) = M(v)$  otherwise. Now let  $D_+(\cdot)$  be the one sided derivative with respect to  $t$  as  $t \searrow 0$ .

Since  $U$  separates  $A$  from  $B$ , we have  $l_{M_t}(A, B) \geq (l_M(A, B) + t)$  so that

$$D_+(l_{M_t}(A, B)) \geq D_+(l_M(A, B) + t) = 1. \quad (2.2.4)$$

For the norm we have

$$\begin{aligned} D_+(\|M_t\|^p) &= \sum_{v \in V} D_+(M_t(v)^p) \\ &= \sum_{v \in U} D_+((M(v) + t)^p) \\ &= \sum_{v \in U} p(M(v)^{p-1}) = pl_M^*(U) = pl_M^*(A, B). \end{aligned} \quad (2.2.5)$$

Now since  $M$  is extremal we also have

$$\begin{aligned} 0 &\geq D_+(\hat{l}_{M_t}(A, B)) \\ &= D_+\left(\frac{(l_{M_t}(A, B))^p}{\|M_t\|^p}\right) \\ &= \frac{p(l_M(A, B))^{p-1}D_+(l_{M_t}(A, B))\|M\|^p - (l_M(A, B))^pD_+(\|M_t\|^p)}{\|M\|^{2p}} \\ &= \frac{(l_M(A, B))^{p-1}}{\|M\|^{2p}}(pD_+(l_{M_t}(A, B))\|M\|^p - (l_M(A, B))^pD_+(\|M_t\|^p)) \end{aligned}$$

which allows us to conclude

$$0 \geq pD_+(l_{M_t}(A, B))\|M\|^p - l_M(A, B)D_+(\|M_t\|^p). \quad (2.2.6)$$

Substituting (2.2.4) and (2.2.5) into (2.2.6) gives

$$0 \geq p(\|M\|^p - l_M(A, B)l_M^*(A, B))$$

so that

$$l_M(A, B)l_M^*(A, B) \geq \|M\|^p. \quad (2.2.7)$$

Comparing (2.2.1) and (2.2.7) we conclude if  $M$  is extremal, then there is equality in (2.2.1). Equality in (2.2.2) follows by the same argument.

□

It is worth noting that if equality holds in (2.2.1) then each of the inequalities in (2.2.3) must be equality. We can draw two conclusions. First, for an extremal metric  $M$  we have  $l_M^*(U_M(t)) = l_M^*(A, B)$  for all  $t \in [0, l_M(A, B))$ . Second, for every  $v \in V$ , there exists  $t_v \in [0, l_M(A, B))$  such that  $v \in U_M(t_v)$ . Although we will not use either explicitly, it does give a sense of the distribution of an extremal metric.

We are now ready to discuss the algorithm.

### 2.3 The Algorithm

Schramm developed an algorithm for computing an extremal metric on a graph in [Sch93]. He did so to find square tilings associated with graphs. We are interested in extremal metrics as a way to estimate the Ahlfors-regular conformal dimension of graph approximations of the Sierpiński carpet.

Roughly speaking, the idea of the algorithm is to use (2.2.1) as a way to measure the distance a metric is from an extremal metric. At each step, additional mass proportional to the error,  $\|m\|^p - l_m(A, B)l_m^*(A, B)$ , is added to vertices of a separating set and the metric is renormalized.

For a finite graph  $G = (V, E)$  with non-empty subsets  $A, B$  of  $V$ , we now state the algorithm for finding the  $p$ -extremal length.

- (1) For each vertex  $v \in V$  set  $m(v) = (\#V)^{-1/p}$ .
- (2) Find a set  $U \subset V$  that separates  $A$  from  $B$  of least  $m$ -dual-length, let  $l_m^* = l_m^*(U)$ ,  $N = \#U$ , and  $l_m = l_m(A, B)$ .
- (3) If  $l_m^*l_m = \|m\|^p$ , then stop. If equality holds  $m$  is the extremal metric.
- (4) Let  $\tilde{m}(v) = m(v) + \delta$  for vertices  $v$  in the separating set  $U$  and  $\tilde{m}(v) = m(v)$  otherwise, where

$$\delta = \left( \frac{\|m\|^p - l_m^*l_m}{Nl_m} \right)^{\frac{1}{p-1}} \quad (2.3.1)$$

- (5) Replace  $m$  by  $\tilde{m}/\|\tilde{m}\|$  and go to step (2).

There are two changes from Schramm's original algorithm. In step (1) Schramm initially distributed the mass only on one separating set of minimal cardinality. We evenly distribute the initial mass. In the graph approximations we are interested in the first iterations would tend to roughly distribute the mass evenly to the vertices, so that change was made. In step (4) we use a slightly smaller value of  $\delta$  so that the subsequent proofs follow. Specifically, Schramm has  $(Nl_m - l_m^*)$  in the denominator where we have only  $Nl_m$ .

The obvious question is the convergence of the algorithm to an extremal metric. We address that now. We will let  $G = A_n$  with distinguished non-empty subsets

$A, B \subset V$  taken to be  $T_n, B_n \subset V_n$ . Restrictions on  $p$  will often be necessary as well. Before we proceed with the discussion of the algorithm, we pause to look at two useful analysis lemmas.

**Lemma 2.3.1.** *For  $1 < p < 2$  and  $x > 0$ , we have*

$$(1 + x)^p < 1 + px + x^p. \quad (2.3.2)$$

*Proof.* A routine calculus argument will suffice. To that end, let  $f(x) = (1 + x)^p$  and  $g(x) = 1 + px + x^p$ . It is clear that  $f(0) = g(0)$ , so (2.3.2) will follow from  $\frac{d}{dx}(f(x) - g(x)) < 0$  for  $x > 0$ .

Case 1: for  $0 < x < 1$

$$\begin{aligned} \frac{d}{dx}(f(x) - g(x)) &= p [(1 + x)^{p-1} - (1 + x^{p-1})] \\ &< p [(1 + x)^{p-1} - (1 + x)] \\ &< 0 \end{aligned}$$

Case 2: for  $x \geq 1$

$$\begin{aligned} \frac{d}{dx}(f(x) - g(x)) &= p [(1 + x)^{p-1} - (1 + x^{p-1})] \\ &< p [(1 + x)^{p-1} - ((p - 1) + x^{p-1})] \\ &\leq p [(1 + x)^{p-1} - ((p - 1)x^{p-2} + x^{p-1})] \\ &< 0 \end{aligned}$$

The final inequality is due to  $((p - 1)x^{p-2} + x^{p-1})$  being the linear approximation of  $(\cdot)^{p-1}$  based at  $x$ , evaluated at  $x + 1$ , which overestimates  $(1 + x)^{p-1}$  since  $(\cdot)^{p-1}$  is concave down, see Figure 2.4.

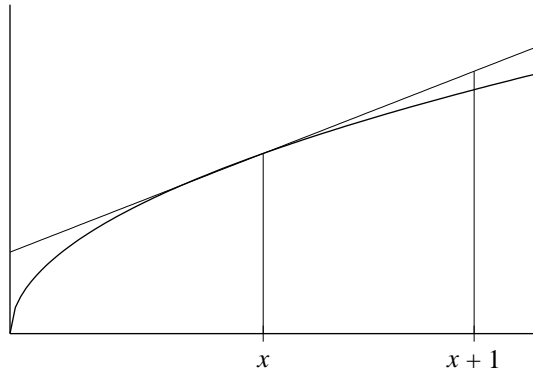


Figure 2.4: The linear approximation of  $(\cdot)^{p-1}$  based at  $x$

□

**Lemma 2.3.2.** For  $p > 1$ , and  $x, c > 0$ , we have

$$(x + c)^p > x^p + pcx^{p-1} \quad (2.3.3)$$

*Proof.* Another routine calculus argument will verify this inequality. Let  $f(c) = (x + c)^p$  and  $g(c) = x^p + pcx^{p-1}$ . It is clear that  $f(0) = g(0)$ , so (2.3.3) will follow from  $\frac{d}{dc}(f(c) - g(c)) > 0$  for  $c > 0$ .

$$\begin{aligned} \frac{d}{dc}(f(c) - g(c)) &= p(x + c)^{p-1} - px^{p-1} \\ &= p[(x + c)^{p-1} - x^{p-1}] \\ &> 0 \end{aligned}$$

□

With the initial inequalities proven, we can turn our attention to the algorithm itself. In the following statement and proof we suppress the dependence on the sets  $A$  and  $B$  and write  $l_m$  for  $l_m(A, B)$ ,  $\hat{l}_m$  for  $\hat{l}_m(A, B)$ , and  $l_m^*$  for  $l_m^*(A, B)$ .

**Lemma 2.3.3.** *Each time the algorithm reaches step (4) we have*

$$\|\tilde{m}\|^p < \|m\|^p + p\delta l_m^* + N\delta^p, \quad (2.3.4)$$

and

$$\hat{l}_{\tilde{m}} - \hat{l}_m > \frac{\delta l_m^{p-1} (p-1) (\|m\|^p - l_m^* l_m)}{\|m\|^p (\|m\|^p + p\delta l_m^* + N\delta^p)} > 0. \quad (2.3.5)$$

*Proof.* We use (2.3.2) to verify (2.3.4).

$$\begin{aligned} \|m^*\|^p &= \sum_{v \in V} m(v)^p = \sum_{v \notin U} m(v)^p + \sum_{v \in U} (m(v) + \delta)^p \\ &\leq \sum_{v \notin U} m(v)^p + \sum_{v \in U} m(v)^p \left(1 + \frac{\delta}{m(v)}\right)^p \\ &< \sum_{v \notin U} m(v)^p + \sum_{v \in U} m(v)^p \left[1 + p\frac{\delta}{m(v)} + \left(\frac{\delta}{m(v)}\right)^p\right] \\ &\leq \sum_{v \notin U} m(v)^p + \sum_{v \in U} m(v)^p + p\delta \sum_{v \in U} m(v)^{p-1} + \sum_{v \in U} \delta^p \\ &\leq \|m\|^p + p\delta l_m^* + N\delta^p \end{aligned}$$

Now use (2.3.4) and Lemma 2.3.2 to proceed as follows.

$$\begin{aligned} \hat{l}_{\tilde{m}} - \hat{l}_m &= \frac{(l_m + \delta)^p}{\|\tilde{m}\|^p} - \frac{l_m^p}{\|m\|^p} \\ &> \frac{(l_m + \delta)^p}{\|m\|^p + p\delta l_m^* + N\delta^p} - \frac{l_m^p}{\|m\|^p} \\ &> \frac{l_m^p + p\delta l_m^{p-1}}{\|m\|^p + p\delta l_m^* + N\delta^p} - \frac{l_m^p}{\|m\|^p} \\ &\geq \frac{\|m\|^p p\delta l_m^{p-1} - p\delta l_m^* l_m^p - N\delta^p l_m^p}{\|m\|^p (\|m\|^p + p\delta l_m^* + N\delta^p)} \\ &\geq \frac{\delta l_m^{p-1} [p(\|m\|^p - l_m^* l_m) - N\delta^{p-1} l_m]}{\|m\|^p (\|m\|^p + p\delta l_m^* + N\delta^p)} \end{aligned}$$

Substituting the value of  $\delta$  and simplifying we have (2.3.5).  $\square$

**Lemma 2.3.4.** *For  $c_1, a_n > 0$  and  $\beta \geq 2$ , if  $a_n - a_{n+1} \geq c_1 a_n^\beta$  then there exists  $c_2$  such that  $a_n \leq c_2 n^{\frac{1}{1-\beta}}$ .*

*Proof.* Initially we note that  $a_n - a_{n+1} \geq c_1 a_n^\beta$  implies

$$a_{n+1} \leq a_n(1 - c_1 a_n^{\beta-1}) \quad (2.3.6)$$

$$a_{n+1} \leq a_n \quad (2.3.7)$$

Now choose  $c_2 = \max \left\{ a_1, c_1^{\frac{1}{1-\beta}} \right\}$ . The proof then proceeds by induction. By our choice of  $c_2$  it is clear that  $a_1 \leq c_2$ . Now assume  $a_n \leq c_2 n^{\frac{1}{1-\beta}}$ .

Case 1: if  $a_n \leq c_2(n+1)^{\frac{1}{1-\beta}}$ , then by (2.3.7) we have  $a_{n+1} \leq c_2(n+1)^{\frac{1}{1-\beta}}$ .

Case 2: if  $c_2(n+1)^{\frac{1}{1-\beta}} < a_n \leq c_2 n^{\frac{1}{1-\beta}}$ , then using (2.3.6), our choice of  $c_2$ , and the observation that for  $\beta \geq 2$  and  $0 < x < 1$ ,  $x \leq x^{\frac{1}{\beta-1}}$  we have

$$\begin{aligned} a_{n+1} &\leq a_n(1 - c_1 a_n^{\beta-1}) \leq c_2 n^{\frac{1}{1-\beta}} \left( 1 - c_1 \left( c_2(n+1)^{\frac{1}{1-\beta}} \right)^{\beta-1} \right) \\ &\leq c_2 n^{\frac{1}{1-\beta}} \left( 1 - \frac{1}{n+1} \right) \\ &\leq c_2 n^{\frac{1}{1-\beta}} \left( 1 - \frac{1}{n+1} \right)^{\frac{1}{\beta-1}} \\ &\leq c_2 n^{\frac{1}{1-\beta}} \left( \frac{n}{n+1} \right)^{\frac{1}{\beta-1}} \\ &\leq c_2 n^{\frac{1}{1-\beta}} \left( \frac{n+1}{n} \right)^{\frac{1}{1-\beta}} \\ &= c_2(n+1)^{\frac{1}{1-\beta}} \end{aligned}$$

$\square$

In the following arguments, it will be useful to denote the metric in the  $j$ -th

iteration as  $m(j)$ ; we also write  $N_j$  for  $\#U$  found in step (2). Again we suppress the dependence on  $A$  and  $B$  in  $l_m(A, B)$  and  $\hat{l}_m(A, B)$ .

**Lemma 2.3.5.** *For the graph approximation  $A_n$ ,  $n \geq 0$ , and  $p > \frac{3}{2}$ , every time the algorithm reaches step (4) we have*

$$N_j l_{m(j)} > 1 \tag{2.3.8}$$

$$\delta = \left( \frac{\|m(j)\|^p - l_{m(j)}^* l_{m(j)}}{N_j l_{m(j)}} \right)^{\frac{1}{p-1}} \in [0, 1) \tag{2.3.9}$$

*Proof.* Since the mass is initially evenly distributed, for the first iteration we know that  $N = \#D_n = 2^{n+1}$  by Lemma 2.1.3. Additionally, the initial  $m$ -length is simply the product of the number of vertices in a shortest vertical path and the initial mass of each vertex. By (2.1.3),  $\#V \leq (3^n + 1)^2$ , so that

$$l_{m(1)} = (3^n + 1)(\#V^{-1/p}) \geq \frac{3^n + 1}{(3^n + 1)^{2/p}}.$$

Limiting our attention to the case where  $p > \frac{3}{2}$  we have

$$N_1 l_{m(1)} \geq \frac{(2^{n+1})(3^n + 1)}{(3^n + 1)^{4/3}} = \frac{2^{n+1}}{(3^n + 1)^{1/3}} > 1. \tag{2.3.10}$$

To show  $N_j l_{m(j)} > 1$  for  $j > 1$  we note two things. First, by Lemma 2.1.3,  $N_j \geq 2^{n+1} = N_1$  for every iteration. Second, because  $\tilde{m}(j)$  and  $m(j+1)$  coincide up to scaling,  $\hat{l}_{m(j+1)} = \hat{l}_{\tilde{m}(j)}$ . Additionally, by (2.3.5) we have  $\hat{l}_{m(j+1)} > \hat{l}_{m(j)}$ . Since  $\|m(j+1)\| = \|m(j)\| = 1$  by construction, it follows that  $l_{m(j+1)} > l_{m(j)}$ . By induction we have  $l_{m(j)} > l_{m(1)}$ . Taken together with (2.3.10) we have  $N_j l_{m(j)} > N_1 l_{m(1)} > 1$  for all iterations  $j$ , verifying (2.3.8)

(2.3.9) follows directly from (2.3.8) and (2.2.1) since  $\|m\| = 1$ .  $\square$

**Theorem 2.3.6.** *For the graph approximation  $A_n = (V_n, E_n)$  when  $n \geq 1$  and  $\frac{3}{2} < p < 2$ , the algorithm converges to the extremal metric  $M$  with  $\|M\| = 1$ . Additionally, the normalized length converges to the  $p$ -extremal length  $\hat{l}_M(A, B)$ . Specifically, for  $j \in \mathbb{N}$ , and positive constants  $C_1 = C(p, \#V_n, L)$  and  $C_2 = C(p, \#V_n, L)$*

$$\|M - m(j)\| \leq C_1 j^{(1-p)/2} \quad (2.3.11)$$

$$\hat{l}_M - \hat{l}_{m(j)} \leq C_2 j^{1-p} \quad (2.3.12)$$

*Proof.* For simplification of the notation, we suppress the dependence on the sets  $A$  and  $B$ . We start by showing (2.3.12) holds. Let  $\varepsilon(j) = 1 - \frac{\hat{l}_{m(j)}}{\hat{l}_M}$ . Then by (2.3.5) we have

$$\begin{aligned} \varepsilon(j) - \varepsilon(j+1) &\geq \frac{\hat{l}_{m(j+1)} - \hat{l}_{m(j)}}{\hat{l}_M} \\ &\geq \frac{\delta l_m^{p-1} (p-1) (\|m\|^p - l_m^* l_m)}{L \|m\|^p (\|m\|^p + p\delta l_m^* + N\delta^p)} \end{aligned}$$

Above, and in subsequent statements, the explicit dependence on  $j$  in  $m(j)$  is suppressed and we write only  $m$ . We do so since  $m(j+1)$  no longer plays a role. In our case  $\|m\|^p = 1$  and  $\frac{3}{2} < p < 2$ , so we can simplify slightly.

$$\begin{aligned} \varepsilon(j) - \varepsilon(j+1) &\geq \frac{\delta l_m^{p-1} (p-1) (1 - l_m^* l_m)}{\hat{l}_M (1 + p\delta l_m^* + N\delta^p)} \\ &\geq \frac{\delta l_m^{p-1} (1 - l_m^* l_m)}{2\hat{l}_M (1 + 2\delta l_m^* + N\delta^p)} \end{aligned}$$

We make use of a number of inequalities to continue. We have  $Nl_m > 1$  by (2.3.8) and  $\delta = \left(\frac{1 - l_m^* l_m}{Nl_m}\right)^{\frac{1}{p-1}} < 1$  by (2.3.9). We also use the obvious, and very coarse estimates that  $1, l_m$ , and  $N$  are each smaller than  $\#V$ .  $l_m^* < \#V$  follows from

$\|m\| = 1$ . Finally,  $\frac{3}{2} < p < 2$  implies  $1 < \frac{1}{p-1} < 2$  so we further estimate

$$\begin{aligned}
\varepsilon(j) - \varepsilon(j+1) &\geq \left( \frac{1 - l_m^* l_m}{N l_m} \right)^{\frac{1}{p-1}} \frac{l_m^{p-1} (1 - l_m^* l_m)}{2 \hat{l}_M (1 + 2l_m^* + N)} \\
&\geq \left( \frac{1 - l_m^* l_m}{N l_m} \right)^{\frac{1}{p-1}} \frac{l_m^{p-1} (1 - l_m^* l_m)}{8 \hat{l}_M \#V} \\
&\geq \frac{(1 - l_m^* l_m)^{\frac{p}{p-1}}}{8 \hat{l}_M \#V N^2 l_m^{3-p}} \\
&\geq \frac{l_m^p (1 - l_m^* l_m)^{\frac{p}{p-1}}}{\hat{l}_M 8 \#V^3 l_m^3} \\
&\geq (1 - \varepsilon(j)) \frac{(1 - l_m^* l_m)^{\frac{p}{p-1}}}{8 \#V^3 \hat{l}_M^3} \\
&\geq \frac{(1 - \varepsilon(1))}{8 \#V^3 \hat{l}_M^3} \left( 1 - ((l_m^* l_m)^p)^{\frac{1}{p}} \right)^{\frac{p}{p-1}}.
\end{aligned}$$

Since  $\|m\| = 1$ , (2.2.2) implies  $(l_m^*)^p \leq \frac{1}{\hat{l}_M}$ . Now letting  $C_1 = \frac{(1 - \varepsilon(1))}{8 \#V^3 \hat{l}_M^3}$  we have

$$\begin{aligned}
\varepsilon(j) - \varepsilon(j+1) &\geq C_1 \left( 1 - \left( \frac{l_m^p}{\hat{l}_M} \right)^{\frac{1}{p}} \right)^{\frac{p}{p-1}} \\
&= C_1 \left( 1 - (1 - \varepsilon(j))^{\frac{1}{p}} \right)^{\frac{p}{p-1}} \\
&\geq C_1 (\varepsilon(j))^{\frac{p}{p-1}}.
\end{aligned}$$

Since  $\frac{3}{2} < p < 2$  implies  $2 < \frac{p}{p-1} < 3$ , Lemma 2.3.4 applies and (2.3.12) follows.

We now turn our attention to showing (2.3.11). We start by showing convergence of the metric using an argument by contradiction. Assume that  $m(j) \not\rightarrow M$ . Then, for some  $\epsilon > 0$  we choose a subsequence  $m(j_k)$  such that  $\|m(j_k) - M\| > \epsilon$  for each  $k$ . Since  $0 \leq m(j_k)(v) \leq \|m(j_k)\| = 1$  for each vertex  $v \in V_n$ ,  $m(j_k)$  is a bounded sequence in  $\mathbb{R}^{\#V_n}$ . The Bolzano-Weierstrass theorem then applies and we can find a convergent subsequence  $m(j_{k_m}) \rightarrow M^*$ . By (2.3.12) we have  $\hat{l}(m(j_{k_m})) \rightarrow \hat{l}_M$ . Since  $\hat{l}$

is a composition of continuous functions, it is a continuous function on  $\mathbb{R}^{\#V_n}$ , allowing us to conclude that  $\hat{l}_{M^*} = \hat{l}_M$ . By the uniqueness of the extremal metric, Theorem 2.2.3, we have  $M^* = M$ . Arriving at a contradiction, we conclude that  $m(j) \rightarrow M$ .

With convergence established, we turn our attention to the rate of convergence. Our first step will be to scale the metric; let  $m'(j) = m(j) \left( \frac{\hat{l}_M}{\hat{l}_{m(j)}} \right)^{1/p}$ . As before, we will suppress the dependence on  $j$  and write only  $m'$ . It is worth noting that  $\hat{l}_M \geq \hat{l}_m > 0$  so that  $\frac{\hat{l}_M}{\hat{l}_m} \geq 1$ . Additionally, since  $\frac{1}{2} < \frac{1}{p} < \frac{2}{3}$ , we have

$$\left( \frac{\hat{l}_M}{\hat{l}_m} \right)^{1/p} < \frac{\hat{l}_M}{\hat{l}_m}. \quad (2.3.13)$$

By (2.3.12) we have

$$\frac{\hat{l}_M}{\hat{l}_m} \leq 1 + \frac{C_2}{\hat{l}_m} j^{1-p}.$$

We will be using this inequality frequently in the following argument; to simplify notation, let

$$\epsilon := \frac{C_2}{\hat{l}_m} j^{1-p}.$$

So that

$$\frac{\hat{l}_M}{\hat{l}_m} \leq 1 + \epsilon. \quad (2.3.14)$$

We initially apply the triangle inequality and the definition of  $m'$  to see

$$\begin{aligned} \|M - m\| &\leq \|M - m'\| + \|m' - m\| \\ &= \|M - m'\| + \|m\| \left( \left( \frac{\hat{l}_M}{\hat{l}_m} \right)^{1/p} - 1 \right) \end{aligned}$$

Now applying (2.3.13) and then (2.3.12) and  $\|m\| = 1$  we have

$$\begin{aligned} \|M - m\| &\leq \|M - m'\| + \|m\| \left( \frac{\hat{l}_M}{\hat{l}_m} - 1 \right) \\ &= \|M - m'\| + \epsilon. \end{aligned} \tag{2.3.15}$$

To estimate  $\|M - m'\|$  we apply Hanner's inequality for  $L^p$  spaces in the case where  $p \in [1, 2]$  [Han56]. As a reminder, all norms we consider are assumed to be  $p$ -norms, for a fixed  $p \in (3/2, 2)$ ; specifically,  $\|\cdot\| = \|\cdot\|_p$  in the following:

$$2^p (\|F\|^p + \|G\|^p) \geq (\|F + G\| + \|F - G\|)^p + \left| \|F + G\| - \|F - G\| \right|^p \tag{2.3.16}$$

We will want to approach each side of the inequality separately with  $F = M/2$  and  $G = m'/2$ . Starting with the left hand side, we have the following.

$$2^p (\|F\|^p + \|G\|^p) \leq 2^p \left( \frac{1}{2^p} + \frac{1}{2^p}(1 + \epsilon) \right) = 2 + \epsilon \tag{2.3.17}$$

The right hand side is more delicate. We start by showing that  $\|F + G\| \geq 1$ . Let  $\gamma \in \Gamma(A, B)$ , i.e.  $\gamma$  is a path from  $A$  to  $B$ , since  $\|M\| = \|m\| = 1$ ,  $M$  is a metric with  $l_M(\gamma) \geq \hat{l}_M^{1/p}$  and  $m$  is a metric with  $l_m(\gamma) \geq \hat{l}_m^{1/p}$ . By the scaling invariance of the normalized length,  $\hat{l}_m$ , we have  $m'$  is a metric with  $l_{m'}(\gamma) \geq \hat{l}_m^{1/p} \left( \frac{\hat{l}_M}{\hat{l}_m} \right)^{1/p} = \hat{l}_M^{1/p}$ , for any path  $\gamma \in \Gamma$ . Now,  $(M + m')/2$  is a metric with  $l_{(M+m')/2}(\gamma) \geq \hat{l}_M^{1/p}$ , for any path  $\gamma \in \Gamma(A, B)$ . Since the extremal length is a supremum over all metrics of positive  $p$ -norm, we have

$$\hat{l}_M \geq \hat{l}((M + m')/2) \geq \frac{(\hat{l}_M^{1/p})^p}{\|(M + m')/2\|^p}$$

allowing us to conclude that

$$\|F + G\|^p = \|(M + m')/2\|^p \geq 1 \quad (2.3.18)$$

A minor adjustment to (2.3.18) allows us to write  $\|F + G\| \geq 1$  and we proceed as follows.

$$(\|F + G\| + \|F - G\|)^p + \left| \|F + G\| - \|F - G\| \right|^p \geq (1 + \|F - G\|)^p + |1 - \|F - G\||^p$$

Since  $\|F - G\| = \frac{1}{2}\|M - m'\| \rightarrow 0$  as  $j \rightarrow \infty$ , for sufficiently large  $j$  we have  $\frac{1}{2}\|M - m'\| < 1$  and the binomial series representation is valid so that

$$\begin{aligned} (1 + \|F - G\|)^p + (1 - \|F - G\|)^p &= \left[ 1 + p \frac{\|M - m'\|}{2} + \frac{p(p-1)}{2} \frac{\|M - m'\|^2}{4} + \dots \right] \\ &\quad + \left[ 1 - p \frac{\|M - m'\|}{2} + \frac{p(p-1)}{2} \frac{\|M - m'\|^2}{4} - \dots \right] \\ &= 2 \left[ 1 + \frac{p(p-1)}{2} \frac{\|M - m'\|^2}{4} + \dots \right] \\ &\geq 2 + p(p-1) \frac{\|M - m'\|^2}{4}. \end{aligned}$$

Combining the previous two results gives

$$(\|F + G\| + \|F - G\|)^p + \left| \|F + G\| - \|F - G\| \right|^p \geq 2 + p(p-1) \frac{\|M - m'\|^2}{4}. \quad (2.3.19)$$

Substituting each side, (2.3.17) and (2.3.19), into Hanner's inequality, (2.3.16), gives

$$2 + \epsilon \geq 2 + p(p-1) \frac{\|M - m'\|^2}{4},$$

or

$$\|M - m'\| \leq \frac{2}{\sqrt{p(p-1)}} \sqrt{\epsilon}. \quad (2.3.20)$$

Finally, we combine (2.3.15) and (2.3.20) to see that

$$\begin{aligned} \|M - m\| &\leq \frac{2}{\sqrt{p(p-1)}} \sqrt{\epsilon} + \epsilon \\ &\leq \frac{2}{\sqrt{p(p-1)}} \sqrt{\frac{C_2}{\hat{l}_{m(j)}} j^{1-p}} + \frac{C_2}{\hat{l}_{m(j)}} j^{1-p}. \end{aligned}$$

Since  $\#V^{-1/p} \leq \hat{l}_{m(1)} \leq \hat{l}_{m(j)}$  for all  $j \geq 1$  (see the proof of Lemma 2.3.5) we have constants  $c_1(p, \#V_n, \hat{l}_M)$  and  $c_2(p, \#V_n, \hat{l}_M)$  such that

$$\|M - m\| \leq c_1 j^{(1-p)/2} + c_2 j^{1-p} \leq (c_1 + c_2) j^{(1-p)/2}.$$

As a final step, we choose a constant  $C_1(p, \#V_n, \hat{l}_M) \geq (c_1 + c_2)$  large enough so that the inequality remains true until  $j$  is large enough that the binomial series representation is valid.  $\square$

Having shown that the algorithm converges, the task at hand becomes implementing it on the graph approximations of the Sierpiński carpet. We do so in the next chapter.

## RESULTS

In the first chapter we saw that the critical exponent for dimension was the same as for the extremal length and that the sequence of extremal lengths should exhibit a certain monotonicity, see Theorems 1.4.12 and 1.4.13. For exponents too small, the extremal length should decrease to zero as the size of the graph approximation increases. For exponents too large, the extremal length should increase without bound as the size of the graph approximation increases. In the second chapter we developed an algorithm to compute the extremal length in the graph approximations. In this chapter we discuss the nuts and bolts of implementing that algorithm and present a summary of the data generated computationally to provide evidence of the Ahlfors-regular conformal dimension of the Sierpiński carpet. We are interested in determining the exponents that exhibit the expected monotonicity.

### 3.1 Implementation

The algorithm was implemented on  $A_2, A_3, A_4$ , and  $A_5$  for a range of  $p$  values between 1.6 and 2.0 by using computer code written in Python. There were a number of alterations and additions required to convert the algorithm from the previous chapter on graph approximations  $A_n$  into a form a computer was well equipped to handle.

Step (2) of the algorithm requires finding a separating set of minimal  $m$ -dual-length, to do so we use a classic recursive algorithm by Dijkstra, see for example [Sed88, pp.413–418], to locate a shortest path in a graph; however, two minor adjustments must be made. First, Dijkstra’s algorithm is formulated to operate on a graph where length is assigned to edges. Our structure assigns mass to vertices. This problem is easily remedied by simply averaging the mass of the two vertices each edge connects and assigning that mass to the edge as a length. With the exception of the

initial and terminal vertices, a path must enter and then exit each vertex, hence the total mass is appropriate. The initial and terminal vertices are handled appropriately after we address the other difficulty, namely, Dijkstra's algorithm requires a starting vertex and a terminal vertex. Our algorithm looks for a shortest path when the initial vertex is any vertex in the top,  $T_n$ , and the terminal vertex is any vertex in the bottom,  $B_n$ . This is also easily addressed by adding two vertices to the graph. A **top vertex** and a **bottom vertex**. The top vertex is simply a vertex of mass zero with edges from it to each vertex in  $T_n$ , similarly for the bottom vertex. Starting at the top vertex, a path would enter a vertex in  $T_n$ , and leave it, solving the issue of assigning mass to edges. Likewise, the path would end at the bottom vertex after leaving a vertex in  $B_n$ . With the addition of these two vertices and the corresponding edges, we have a graph that we can implement Dijkstra's algorithm on.

In order to find horizontal separating sets we will need additional structure in our graph. Initially we add two side vertices, a **left vertex** and a **right vertex** similar to the top and bottom vertices, and the corresponding **side edges** to connect them to the left and right sides, respectively. Additionally, we will need to add new vertices and corresponding edges to fill in the voids left when we removed subsquares. We add one vertex in each void and refer to it as a **ghost vertex**. From each ghost vertex we add **ghost edges** connecting it to each vertex in the boundary of the void. We will also need to add a **diagonal edge** between every pair of vertices in  $E_n$  such that the distance between the corresponding geometric vertices is  $\sqrt{2}/3^n$ .

We now construct an extended graph approximation  $A_n^* = (V_n^*, E_n^*)$  from  $A_n = (V_n, E_n)$ ; see Figure 3.1. Let  $V_n^*$  be  $V_n$  with the two side vertices and the ghost vertices added; let  $E_n^*$  be  $E_n$  with the side edges, the ghost edges, and the diagonal edges added. We continue to use the notation  $L_n$  to represent the set of vertices along the left side of  $A_n$ , whether it is considered a subset of  $V_n$  or a subset of  $V_n^*$ . Similarly,

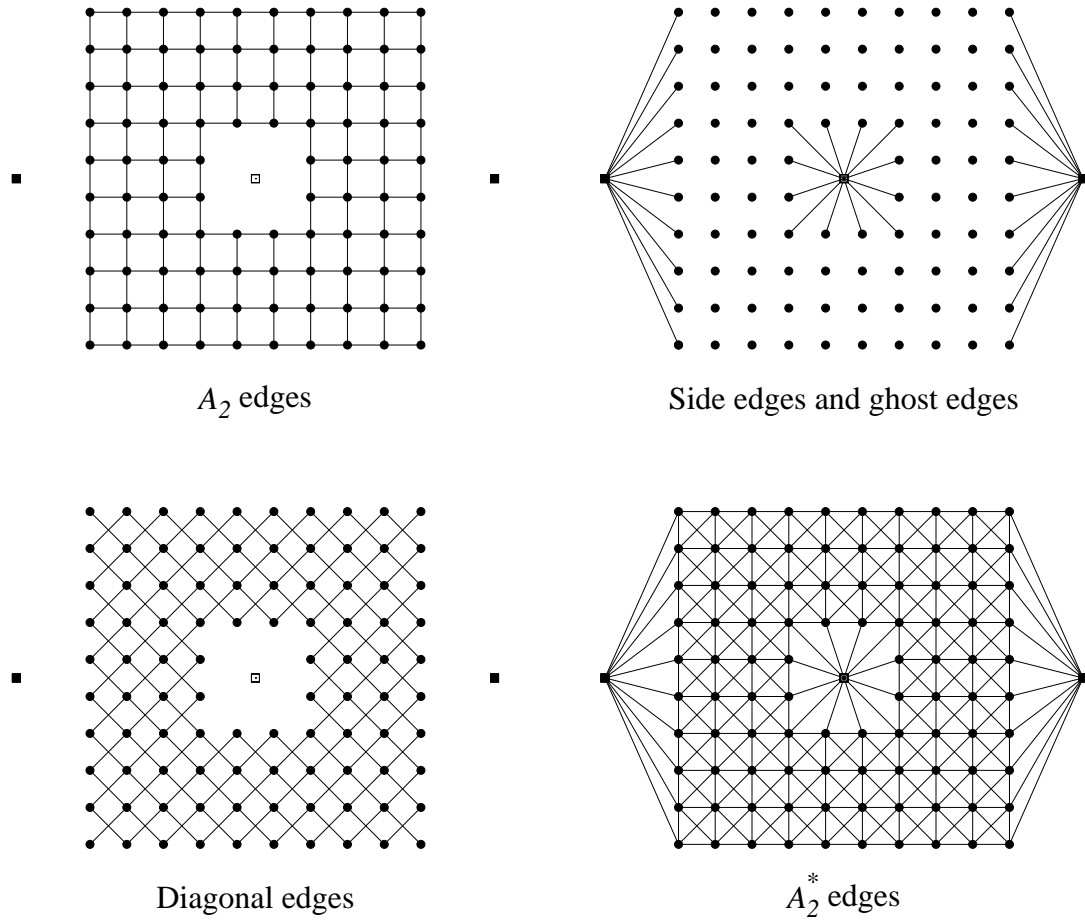


Figure 3.1: Construction of edges in  $A_2^*$ . Side vertices represented as solid squares; the ghost vertex is represented by an open square.

we continue to use  $R_n$ ,  $T_n$ , and  $B_n$  for the right, top, and bottom sides, respectively, regardless of the graph approximation.

We use the language of  $m$ -dual-length for a separating set. The notation would imply that a separating set is a path with 'length'. In the case where the separating set has minimal  $m$ -dual-length, the vertices in the set are exactly the non-ghost, non-side vertices in a path in the extended graph  $A_n^*$ . We show this in Theorem 3.1.1 below.

Before we begin, a note on terminology. In Lemma 2.1.3 we discussed minimal

horizontal separating sets being sets that separated the top from the bottom, hence horizontal, and minimal in the sense of cardinality. Our focus has shifted to horizontal separating sets of minimal  $m$ -dual-length. It is worth noting that although the two may be the same, and initially are since the mass is evenly distributed on the vertices, there is no reason to expect the two ideas to coincide once mass begins to shift. In this chapter all references to minimal separating sets should be understood to be horizontal separating sets of minimal  $m$ -dual-length with no implication regarding cardinality.

The fundamental concept in the subsequent argument is the minimality of the  $m$ -dual-length of the separating set. Since each vertex has positive mass, each vertex in a minimal separating set must be needed in order to separate the top from the bottom.

**Theorem 3.1.1.** *A separating set  $D \subset V_n$  of minimal  $m$ -dual-length is the set of non-ghost, non-side vertices in a path in  $A_n^*$  that connects the left side vertex to the right side vertex.*

*Proof.* Let  $D \subset V_n$  be a minimal separating set. Since  $D$  has minimal  $m$ -dual-length and each vertex in  $V_n$  has positive mass, every vertex in  $D$  must be adjacent in  $A_n$  to a vertex with a path to the top that does not intersect  $D$ , or it must itself be on the top. (Although it is not critical to the following argument, each vertex in  $D$  must also be adjacent in  $A_n$  to a vertex with a path to the bottom that does not intersect  $D$ , or it must itself be on the bottom.)

It will be useful to have an example in mind; see Figure 3.2. In the figure, vertices in the minimal separating set  $D$  are represented by solid squares. Now, let  $P$  be the set of all vertices that have a path in  $A_n \setminus D$  from them to the top; vertices represented by solid circles in the figure. Vertices represented by open circles are vertices that

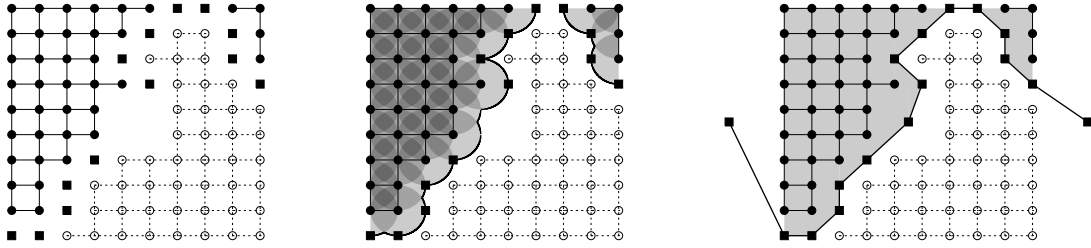


Figure 3.2: A path generated by a minimal  $m$ -dual-length separating set.

connect to the bottom, but do not play a role in the following argument.

Since  $D$  is a separating set, every vertex in the top  $T_n$  is either in  $D$  or is in  $P$ . If  $P = \emptyset$ , then  $D = T_n$ , and there is a clear path from the left to the right formed from the vertices in the top since there are edges between them. If  $P \neq \emptyset$ , around each vertex in  $P$ , place a closed disk of radius  $3^{-n}$ . We consider the union of the closed disks, and, in particular, the boundary of this union.

If the union is connected, then the part of the boundary that is accessible from the bottom forms a continuous curve constructed of arcs of circles that begins either on the left side or the top and continues until it reaches the right side or the top. If the boundary curve does not start on the left side, there are vertices of  $D$  along the top and adding the horizontal line connecting the adjacent vertices in  $D$  along the top will form a connect curve from the left side and along the boundary. Similarly, if the boundary curve does not end on the right side, we add a horizontal line edges along top to connect the boundary curve to the right side. Now, between vertices on the boundary curve that are adjacent in  $A_n^*$  we homotope the part of the boundary from arcs into horizontal, vertical, or diagonal segments corresponding to edges in  $E_n^*$ . If the boundary curve passes through a removed subsquare, we add the appropriate ghost vertex to  $D$  and homotope the boundary curve into segments corresponding to ghost edges. Now, every vertex in  $D$  is either along the top and connected by a

horizontal segment corresponding to horizontal edges, or is adjacent to a vertex in  $P$ , and hence on the boundary of the union. We form a path, i.e. a sequence of vertices, in the obvious way starting with the left side vertex and following along the boundary curve until we reach the right side at which point we add the right side vertex.

If the union is not connected, as in the figure, there are vertices of  $D$  along the top and adding a horizontal segment corresponding to the horizontal edges connecting the adjacent vertices in  $D$  along the top will connect the boundary components accessible from the bottom. With the horizontal segment included, a continuous curve from the left side to the right side is again formed. As above, we form a path from the left vertex to the right vertex in the in the obvious way.

□

### 3.2 Visual Representations of the Algorithm

Before we look at the numerical data too closely, a visual representation is included to get a basic understanding of the mass distributions found as the algorithm is iterated. Figure 3.3 shows the mass distribution as the iterations grow from 10 to 5000 for  $A_4$  for  $p = 1.85$ . This is sequence of figures is representative of the general situation; the distribution changes in a similar way for the other sizes and other values of  $p$ .

In the section 3.4 we will look closely at the results for  $p = 1.70$ ,  $p = 1.75$ , and  $p = 1.80$ . Figures 3.4 through 3.10 show the distribution for these three exponents on the graph approximations  $A_2$ ,  $A_3$ ,  $A_4$ , and  $A_5$ .

### 3.3 Numerical Results

The numerical results offer some compelling data regarding the discrete extremal length for graph approximations of the Sierpiński carpet. We start by examining the

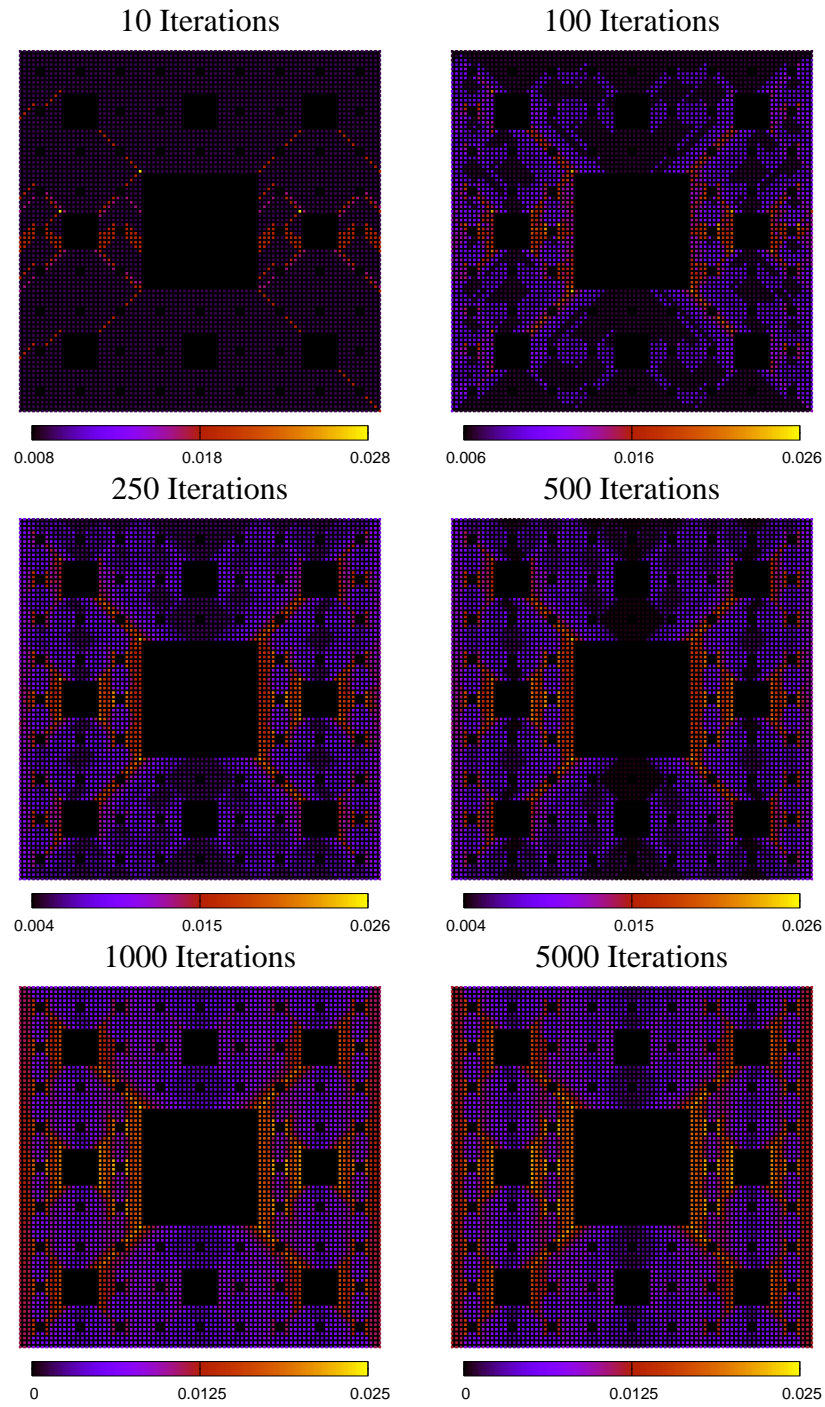


Figure 3.3: Mass distribution on  $A_4$  for  $p = 1.85$  after 10, 100, 250, 500, 1000, and 5000 iterations.

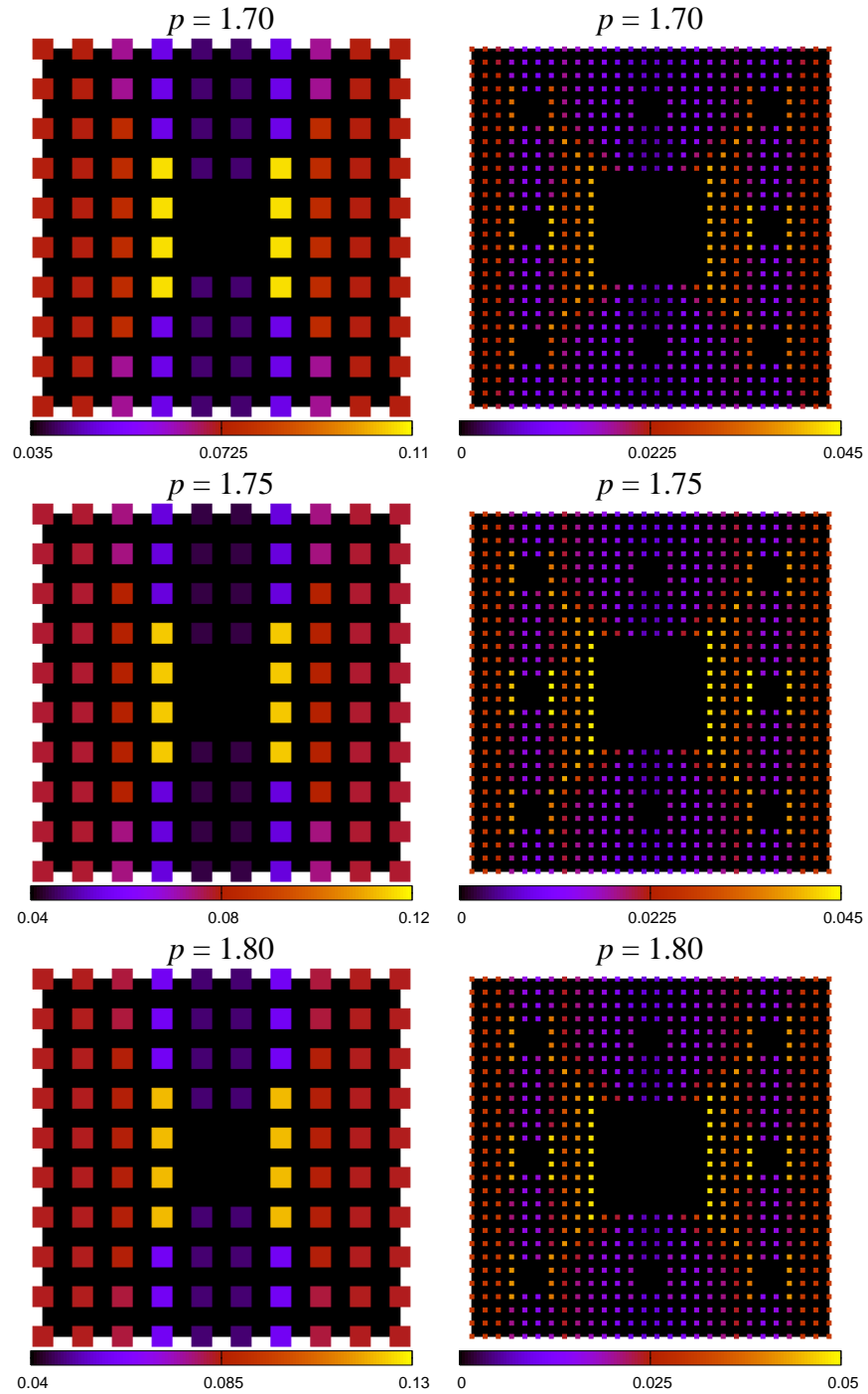


Figure 3.4: Mass distribution on  $A_2$  and  $A_3$  for  $p = 1.70, 1.75,$  and  $1.80$  after 5000 iterations.

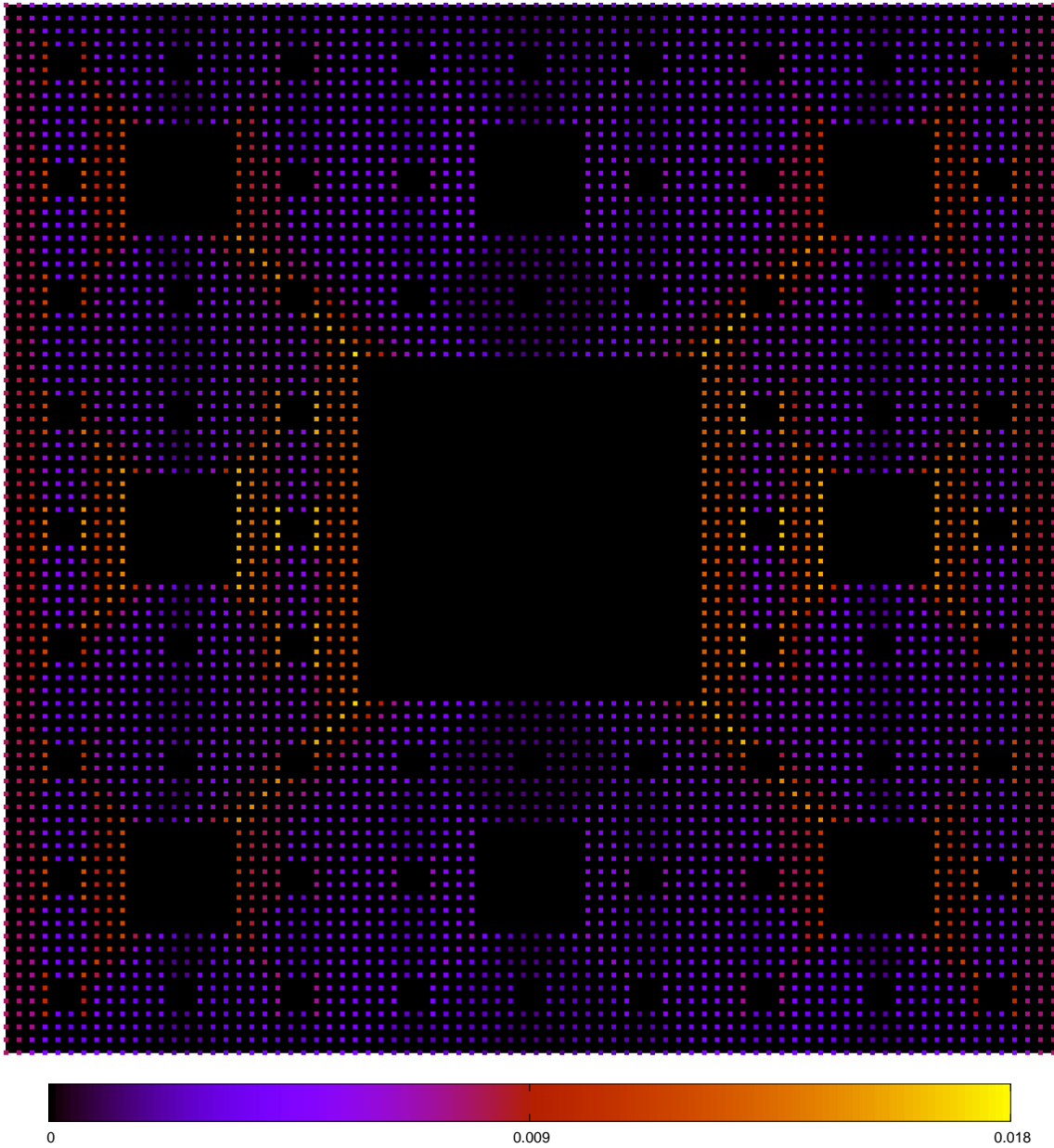


Figure 3.5: Mass distribution on  $A_4$  for  $p = 1.70$  after 5000 iterations.

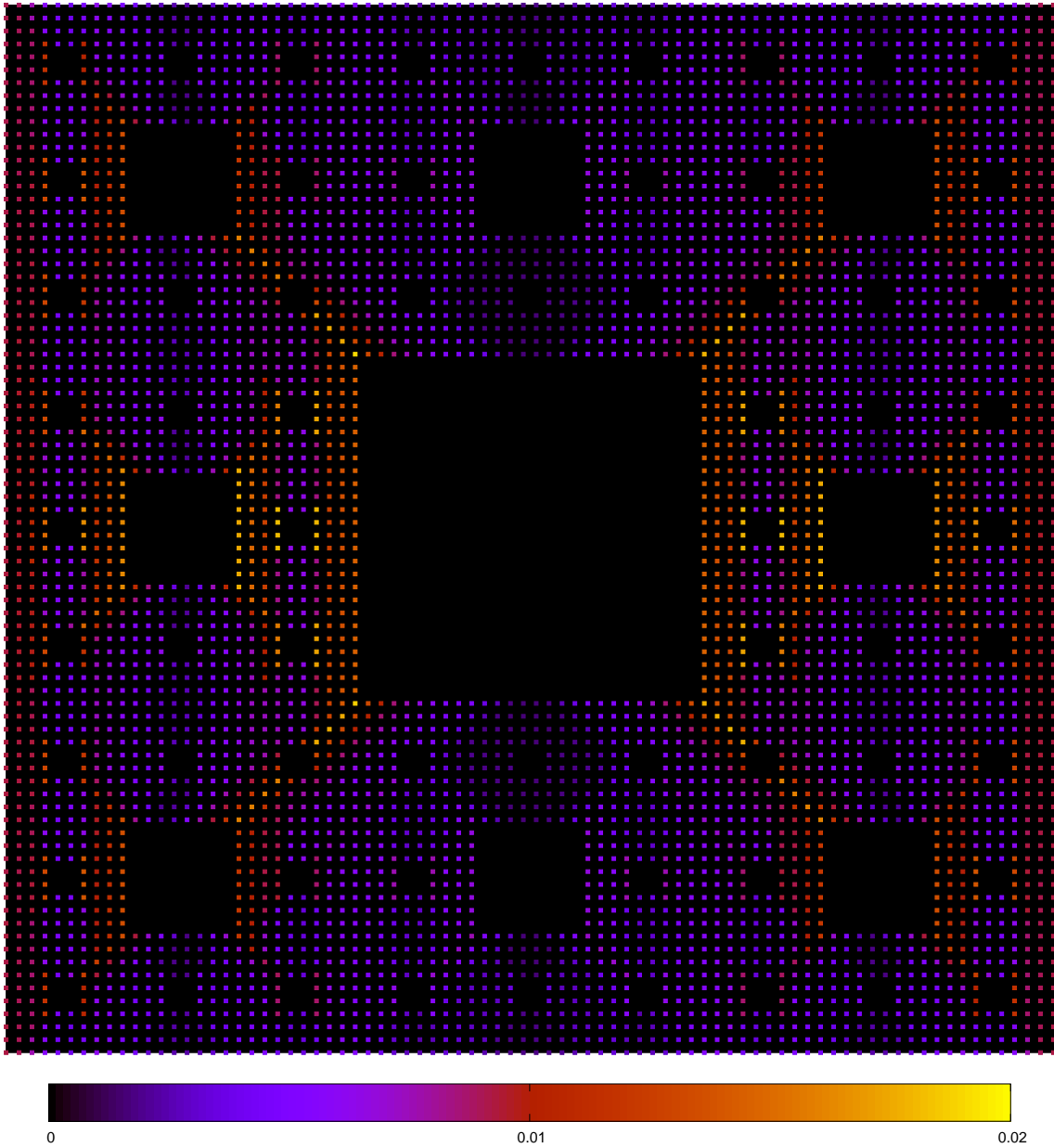


Figure 3.6: Mass distribution on  $A_4$  for  $p = 1.75$  after 5000 iterations.

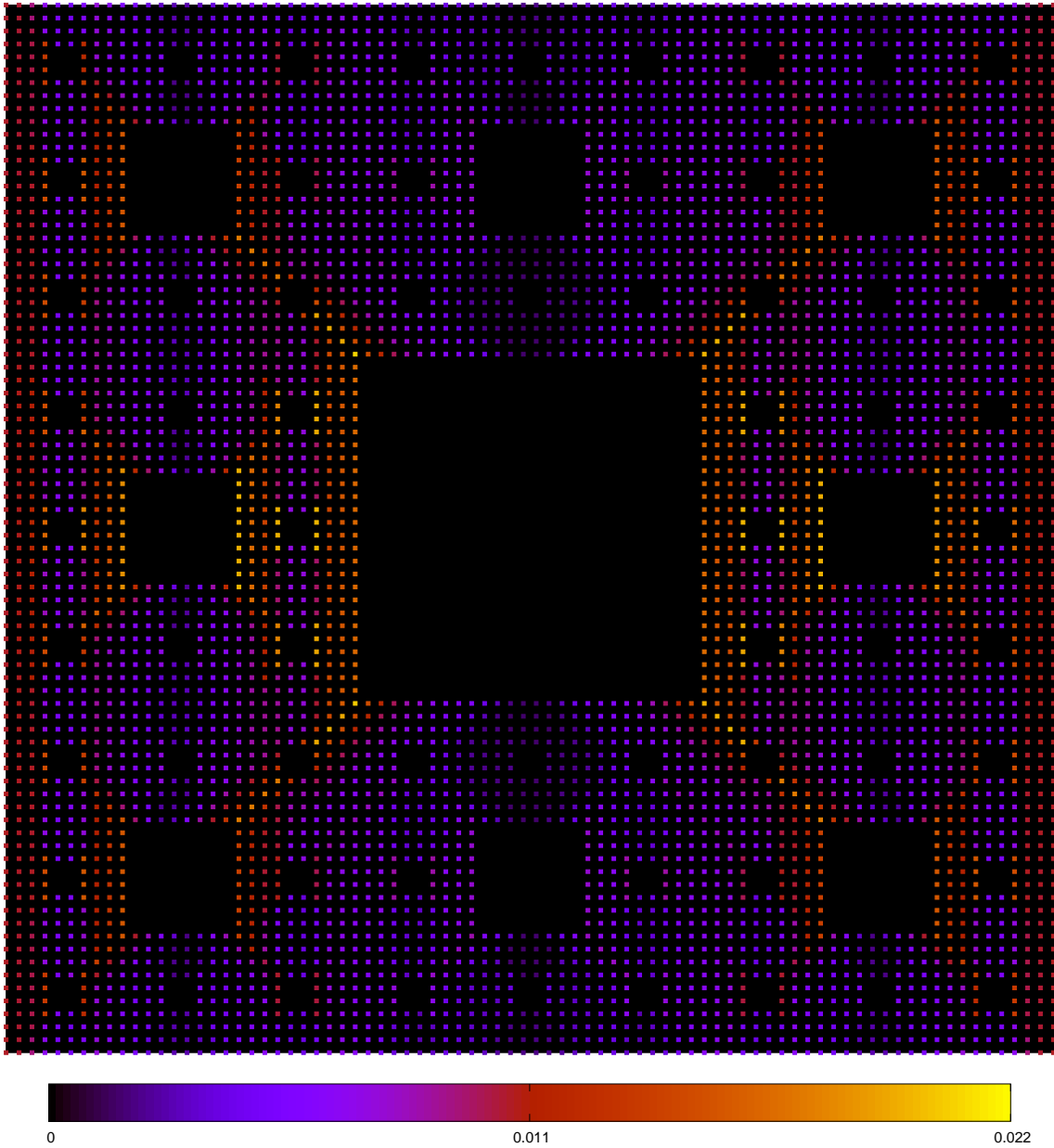


Figure 3.7: Mass distribution on  $A_4$  for  $p = 1.80$  after 5000 iterations.

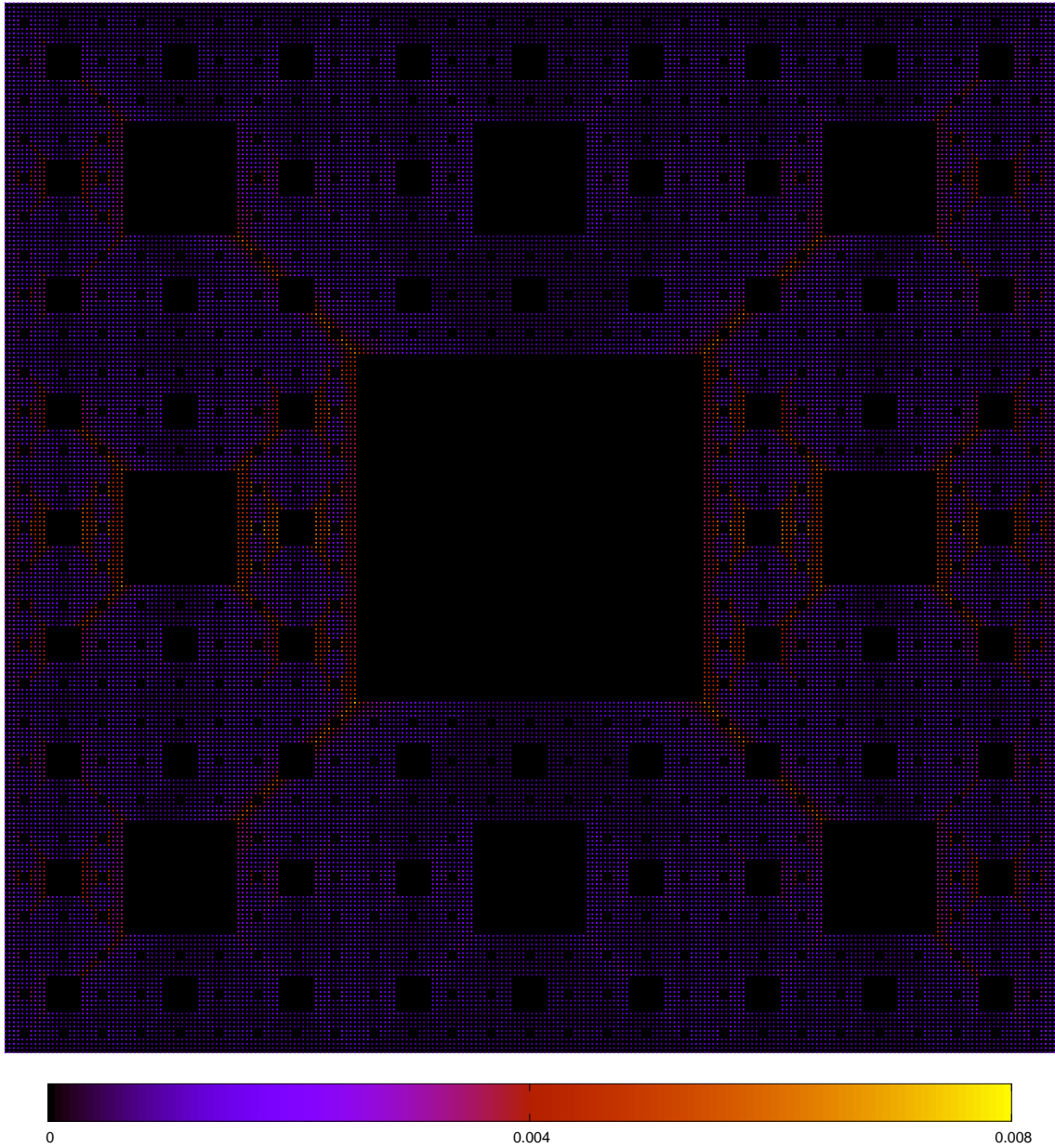


Figure 3.8: Mass distribution on  $A_5$  for  $p = 1.70$  after 2000 iterations.

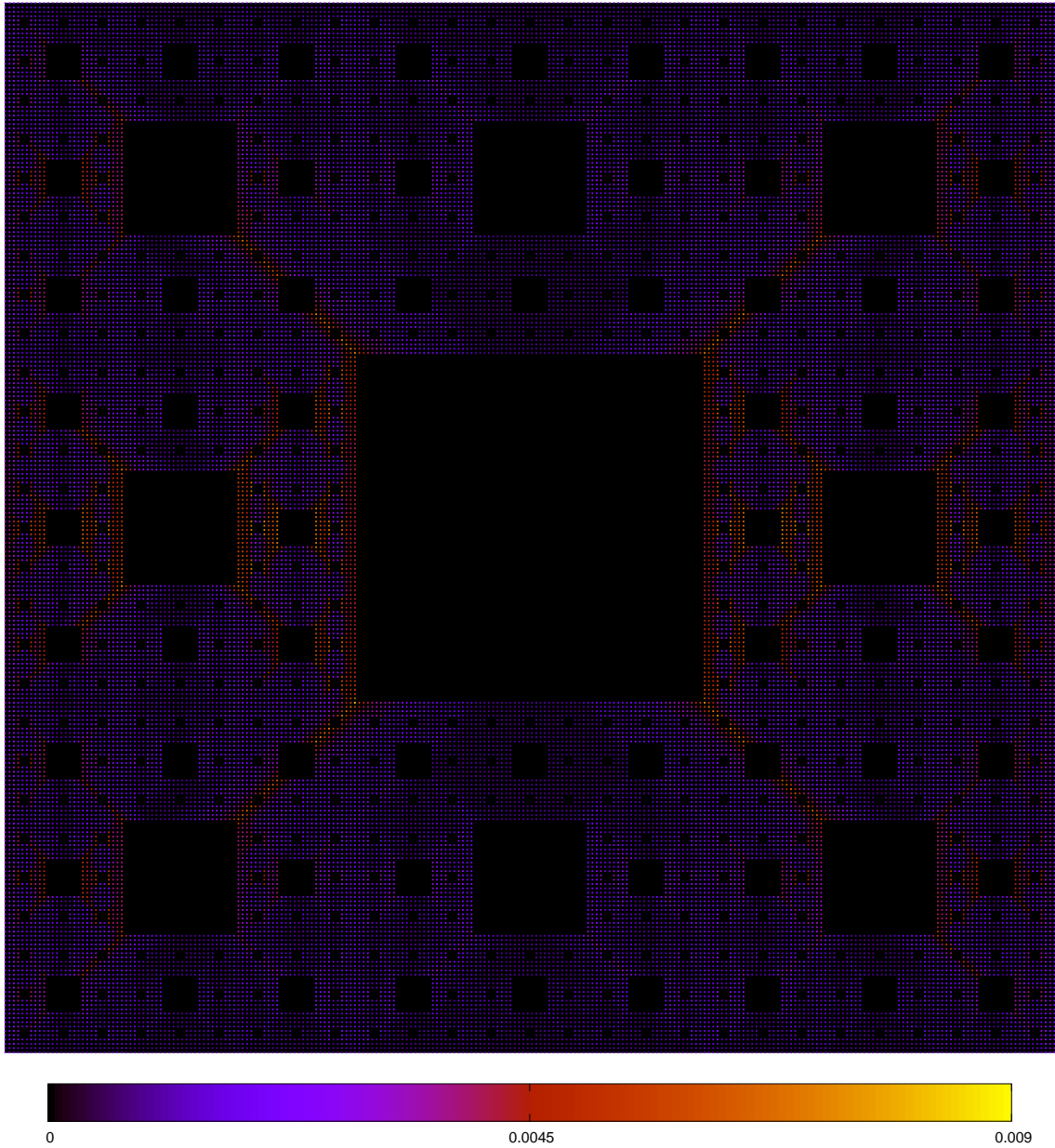


Figure 3.9: Mass distribution on  $A_5$  for  $p = 1.75$  after 2000 iterations.

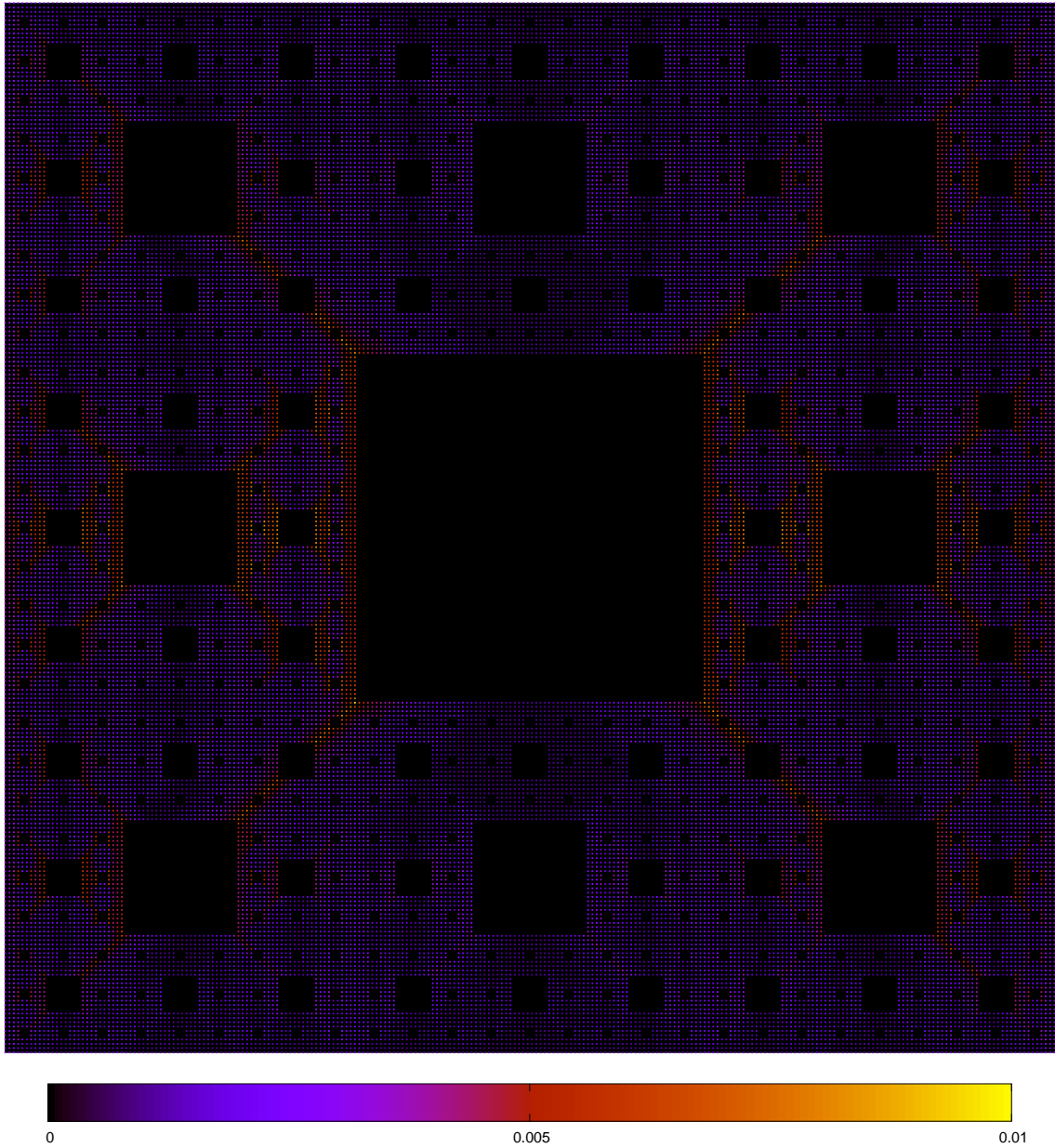


Figure 3.10: Mass distribution on  $A_5$  for  $p = 1.80$  after 2000 iterations.

Iterations	$\hat{l}_n$
1000	0.6332
2500	0.6383
5000	0.6411
10000	0.6431
25000	0.6448
50000	0.6456

Table 3.1: Computed  $\hat{l}_n$  values for  $p = 1.75$  in  $A_2$ .

numerics for  $A_2$ . Since  $A_2$  only has 96 vertices, iterating the algorithm can be performed quickly - on the order of 450,000 iterations per hour - and large data sets can be generated and analyzed before moving forward into larger graph approximations.

The algorithm was applied for  $p$  values in  $\{1.60, 1.65, 1.70, \dots, 1.95, 2.00\}$ . We focus our attention on the case of  $p = 1.75$  for the current discussion, it will prove to be an important exponent in the subsequent discussion. The results for other  $p$  values are very similar.

A summary of the data for  $p = 1.75$  is included in Table 3.1. Denote the normalized length after iteration  $n$  as  $\hat{l}_n$ . Although the sequence  $\{\hat{l}_n\}$  is increasing, the rate of increase slows dramatically as the number of iterations grows.

We would like to be able to project the extremal length  $L$  without iterating an excessive amount of times. In particular, if we let  $\Delta\hat{l}_n := \hat{l}_n - \hat{l}_{n-1}$ , then  $L = \hat{l}_J + \sum_{n=J+1}^{\infty} \Delta\hat{l}_n$ , and the sum becomes the object of interest.

In order to estimate the sum, we estimate the decay rate of  $\Delta\hat{l}_n$  by fitting a line to a graph of  $\log n$  versus  $\log \Delta\hat{l}_n$ . We use a line to fit the log-log plot based on the expected rate of decay we found in (2.3.12). It is clear from Figure 3.11 that the decay rate is significantly higher for the first few iterations than it is in the long term. Ignoring the first 500 iterates gives a better approximation of the decay rate, see Figure 3.12. A least squares fit of the form  $f(x) = mx + b$  was applied to the

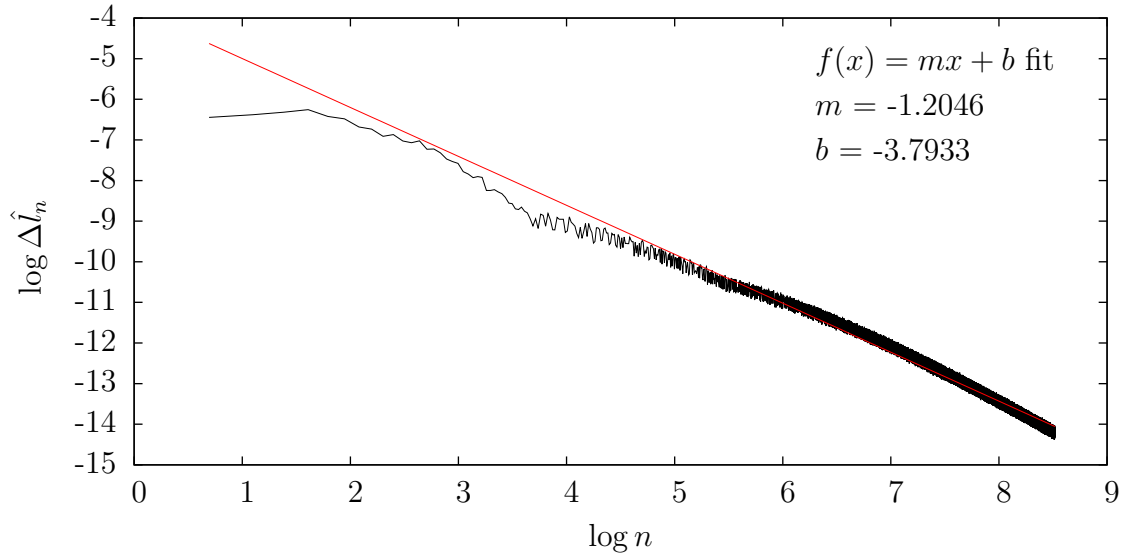


Figure 3.11: Calculating the decay rate of  $\Delta \hat{l}_n$  for  $A_2$  with  $p = 1.75$  for iterations 2-5000.

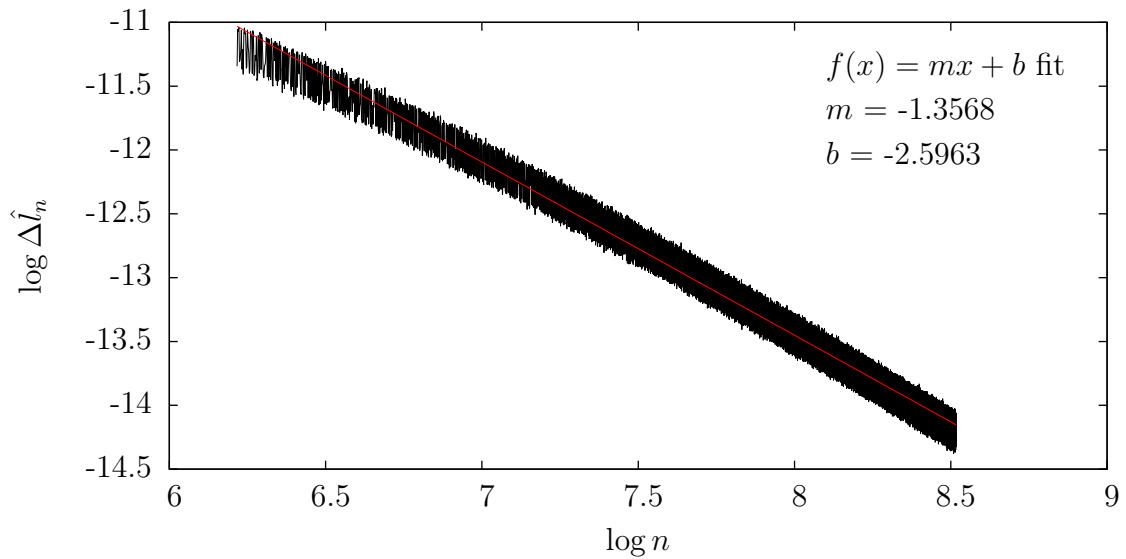


Figure 3.12: Calculating the decay rate of  $\Delta \hat{l}_n$  for  $A_2$  with  $p = 1.75$  for iterations 501-5000.

data.

Once the data were fit we had an estimate of the form  $\log \Delta \hat{l}_n \approx m \log n + b$  giving the following estimate of the extremal length  $L$ , for  $m < -1$ .

$$\begin{aligned} L = \hat{l}_J + \sum_{n=J+1}^{\infty} \Delta \hat{l}_n &\approx \hat{l}_J + e^b \sum_{n=J+1}^{\infty} n^m \\ &\approx \hat{l}_J + e^b \int_J^{\infty} x^m dx \\ &= \hat{l}_J - e^b \frac{J^{m+1}}{m+1} \end{aligned}$$

A similar integral estimate allows us to project the value of  $\hat{l}_K$  for any  $K$  we have interest in. In particular, we can extrapolate the value of  $\hat{l}_{50000}$  as a way to check the validity of our estimates since we have data for that iteration. Data is summarized in Table 3.2. A few things to note initially. As expected, the larger the number of iterations computed the smaller the error. However, the lower part of the table provides the support for the argument that a rather limited subset, only 500 iterations, can provide a useful projection. For  $A_2$  we have the luxury of being able to compute large numbers of iterations. As we start looking at larger graph approximations we will find this beneficial.

The algorithm runs significantly slower on  $A_3$ , on the order of 13,000 iterations per hour. Similar data was generated and is summarized in Table 3.3. Again we see that subsets of 500 iterations are reasonable ways to project the value of  $\hat{l}_{50000}$ .

Based on the stability of the extrapolations in the small cases, we consider the projected values for the extremal length at infinity. In light of Theorem 1.4.12 we are interested not in particular values, but in the trend, i.e. does the value increase or decrease as the size of the graph approximation grows.

The algorithm was not run to a large number of iterations in either the  $A_4$  or  $A_5$

Iterations	$\hat{l}_n$	$m$	$b$	Extrapolated $\hat{l}_{50000}$	% Error
501-1000	0.6332	-1.1419	-4.0662	0.6525	1.061
501-2500	0.6383	-1.2740	-3.1838	0.6482	0.404
501-5000	0.6411	-1.3572	-2.5937	0.6467	0.172
501-10000	0.6431	-1.4252	-2.0817	0.6460	0.063
501-25000	0.6448	-1.4963	-1.5060	0.6457	0.010
1001-1500	0.6356	-1.2864	-3.0732	0.6482	0.405
1501-2000	0.6372	-1.3678	-2.4776	0.6469	0.194
2001-2500	0.6383	-1.4150	-2.1148	0.6463	0.112
2501-3000	0.6391	-1.4349	-1.9582	0.6462	0.086
3001-3500	0.6398	-1.4629	-1.7330	0.6460	0.054
3501-4000	0.6403	-1.4630	-1.7307	0.6460	0.057
4001-4500	0.6407	-1.4428	-1.9019	0.6461	0.072
4501-5000	0.6411	-1.4511	-1.8363	0.6460	0.063

Table 3.2:  $\hat{l}_n$ , curve fitting data, extrapolated  $\hat{l}_{50000}$ , and percent error compared with the computed value of  $\hat{l}_{50000} = 0.6456$  in the projection for various iterations in  $A_2$ .

Iterations	$\hat{l}_n$	$m$	$b$	Extrapolated $\hat{l}_{50000}$	% Error
501-1000	0.6084	-1.2474	-2.6799	0.6395	0.965
501-2500	0.6183	-1.3084	-2.2776	0.6362	0.452
501-5000	0.6239	-1.3445	-2.0197	0.6351	0.278
501-10000	0.6281	-1.3927	-1.6564	0.6342	0.126
501-25000	0.6317	-1.4619	-1.0951	0.6335	0.023
1001-1500	0.6131	-1.3474	-1.9971	0.6348	0.225
1501-2000	0.6161	-1.3138	-2.2366	0.6361	0.424
2001-2500	0.6183	-1.3743	-1.7715	0.6347	0.204
2501-3000	0.6199	-1.3700	-1.8033	0.6348	0.227
3001-3500	0.6212	-1.3959	-1.5742	0.6347	0.208
3501-4000	0.6223	-1.4157	-1.4360	0.6341	0.117
4001-4500	0.6232	-1.4348	-1.2778	0.6339	0.082
4501-5000	0.6239	-1.4859	-0.8468	0.6334	0.003

Table 3.3:  $\hat{l}_n$ , curve fitting data, extrapolated  $\hat{l}_{50000}$ , and percent error compared with the computed value of  $\hat{l}_{50000} = 0.6334$  in the projection for various iterations in  $A_3$ .

$p$	$A_2$		$A_3$		$A_4$
1.60	0.4959	>	0.3970	>	0.3430
1.65	0.5353	>	0.4656	>	0.4252
1.70	0.5850	>	0.5478	>	0.5249
1.75	<b>0.6511</b>	>	<b>0.6444</b>	<	<b>0.6503</b>
1.80	0.7280	<	0.7589	<	0.8061
1.85	0.8155	<	0.8937	<	1.0006
1.90	0.9156	<	1.0535	<	1.2417
1.95	1.0270	<	1.2432	<	1.5429
2.00	1.1515	<	1.4670	<	1.8848

Table 3.4: Projected extremal length for  $A_2$ ,  $A_3$ , and  $A_4$  based off iterations 501-5000.

case due to the time requirements. In the  $A_4$  case the algorithm took on the order of 125 iterations per hour; in the  $A_5$  case the speed dropped to roughly two iterations per hour.

### 3.4 Summary of Data

We consolidate the data in this section and use it to support Conjecture 1.3.18. In particular, we want to apply Theorem 1.4.12. For exponents too small, the extremal length should decrease to zero as the size of the graph approximation increases. For exponents too large, the extremal length should increase without bound as the size of the graph approximation increases.

Before implementing the algorithm on  $A_5$  we want to limit the search for the critical exponent. Tables 3.4 and 3.5 provide strong evidence that the critical exponent is between  $p = 1.70$  and  $p = 1.80$ . In Table 3.4 we use iterations 501 to 5000 to project the extremal length. In Table 3.5 we limit the iterations to 4501 to 5000. Data for other subsets of iterations are similar. In both cases we see a clear trend that for  $p \leq 1.70$  the projected lengths are decreasing as the size of the graph approximation increases. On the other hand, for  $p \geq 1.80$  we see the projected lengths increasing.

$p$	$A_2$		$A_3$		$A_4$
1.60	0.4655	>	0.3901	>	0.3290
1.65	0.5176	>	0.4707	>	0.4170
1.70	0.5786	>	0.5483	>	0.5319
1.75	<b>0.6487</b>	>	<b>0.6380</b>	<	<b>0.6511</b>
1.80	0.7263	<	0.7574	<	0.7985
1.85	0.8169	<	0.8871	<	0.9946
1.90	0.9144	<	1.0491	<	1.2314
1.95	1.0256	<	1.2394	<	1.5312
2.00	1.1507	<	1.4663	<	1.9062

Table 3.5: Projected extremal length for  $A_2$ ,  $A_3$ , and  $A_4$  based off iterations 4501-5000.

We notice that for  $p = 1.75$  the data seems inconclusive. With these projections in mind, we take a close look at the projections for three exponents  $p = 1.70$ ,  $p = 1.75$ , and  $p = 1.80$ . The algorithm was applied to  $A_5$  for each of the three exponents for 2000 iterations.

The numerical evidence from the approximations  $A_2$ ,  $A_3$ ,  $A_4$ , and  $A_5$  strongly suggests that for  $p = 1.70$  the projected extremal lengths are decreasing, see Table 3.6.  $A_2$  iterations 501 to 1000 did not generate a convergent series, hence the  $\infty$  in the table. The important summary of the table is that for any subset of 500 iterations we choose the trend is clear and consistent. The projected length decreases as the size of the approximation increases. In light of Theorem 1.4.12 we claim that  $p = 1.70$  is smaller than the critical exponent, i.e.

$$1.70 < \dim_{AR} S.$$

The numerical evidence also strongly suggests that for  $p = 1.80$  the projected extremal length are increasing, see Table 3.7. The important summary of the table is that for any subset of 500 iterations we choose the trend is again clear and consistent.

Ending Iteration	$A_2$		$A_3$		$A_4$		$A_5$
1000	$\infty$	>	0.5715	>	0.5588	>	0.5292
1500	0.5987	>	0.5507	>	0.5370	>	0.5296
2000	0.5865	>	0.5434	>	0.5414	>	0.5226
2500	0.5825	>	0.5432	>	0.5227		
3000	0.5805	>	0.5538	>	0.5123		
3500	0.5794	>	0.5518	>	0.5117		
4000	0.5788	>	0.5464	>	0.5211		
4500	0.5786	>	0.5423	>	0.5161		
5000	0.5786	>	0.5421	>	0.5319		

Table 3.6: Projected Lengths based off of 500 iterations for  $p = 1.70$ .

Ending Iteration	$A_2$		$A_3$		$A_4$		$A_5$
1000	0.7390	<	0.7640	<	0.8369	<	0.8488
1500	0.7301	<	0.7652	<	0.8189	<	0.8757
2000	0.7281	<	0.7610	<	0.8063	<	0.8484
2500	0.7273	<	0.7575	<	0.8275		
3000	0.7271	<	0.7570	<	0.8224		
3500	0.7269	<	0.7559	<	0.8055		
4000	0.7270	<	0.7543	<	0.7959		
4500	0.7267	<	0.7556	<	0.8004		
5000	0.7263	<	0.7574	<	0.7985		

Table 3.7: Projected Lengths based off of 500 iterations for  $p = 1.80$ .

The projected length increases as the size of the approximation increases. In light of Theorem 1.4.12 we claim that  $p = 1.80$  is larger than the critical exponent, i.e.

$$\dim_{AR} S < 1.80.$$

The data for  $p = 1.75$  are, however, inconsistent, see Table 3.8. Bold entries in the table are values that are particularly troubling insofar as they represent groups of iterations that are inconsistent with similar groups. There is no clear trend, i.e. the lengths are not monotonic as we increase the size of the graph approximation. We

Ending Iteration	$A_2$		$A_3$		$A_4$		$A_5$
1000	0.6797	>	0.6585	<	0.6730	<	0.7107
1500	0.6555	>	0.6439	<	0.6633	<	0.6886
2000	0.6511	>	0.6475	<	<b>0.6725</b>	>	<b>0.6487</b>
2500	0.6496	>	0.6426	<	0.6557		
3000	0.6491	>	<b>0.6429</b>	>	<b>0.6414</b>		
3500	0.6485	>	0.6419	<	0.6481		
4000	0.6485	>	0.6405	<	0.6521		
4500	0.6489	>	0.6397	<	0.6809		
5000	0.6487	>	0.6380	<	0.6511		

Table 3.8: Projected Lengths based off of 500 iterations for  $p = 1.75$ .

saw this in Tables 3.4 and 3.5, and we see it again in closer detail. At this exponent the numerics are simply unstable.

Although we cannot make any claim regarding  $p = 1.75$  we can say that there is strong evidence of our conjecture that

$$1.70 < \dim_{AR} S < 1.80.$$

These bounds are significantly narrower than the rigorous bounds in Corollary 1.3.14 and Theorem 1.3.15.

$$1.6309\dots \approx 1 + \frac{\log 2}{\log 3} \leq \dim_c S \leq \frac{\log\left(\frac{9+\sqrt{41}}{2}\right)}{\log 3} \approx 1.8581\dots$$

## BIBLIOGRAPHY

- [BB90] M. Barlow and R. Bass. “On the resistance of the Sierpinski carpet”. In: *Proceedings of the Royal Society of London. Series A: Mathematical and Physical Sciences* 431.1882 (1990), pp. 345–360.
- [BBS90] M. Barlow, R. Bass, and J. Sherwood. “Resistance and spectral dimension of Sierpinski carpets”. In: *Journal of Physics A: Mathematical and General* 23.6 (1990), p. L253.
- [BT01] Christopher Bishop and Jeremy Tyson. “Locally minimal sets for conformal dimension”. In: *Ann. Acad. Sci. Fenn. Math.* 26.2 (2001), pp. 361–373. ISSN: 1239-629X.
- [BK13] Marc Bourdon and Bruce Kleiner. “Combinatorial modulus, the combinatorial Loewner property, and Coxeter groups”. In: *Groups Geom. Dyn.* 7.1 (2013), pp. 39–107. ISSN: 1661-7207. DOI: 10.4171/GGD/177. URL: <http://dx.doi.org/10.4171/GGD/177>.
- [BP03] Marc Bourdon and Hervé Pajot. “Cohomologie  $l_p$  et espaces de Besov”. In: *J. Reine Angew. Math.* 558 (2003), pp. 85–108. ISSN: 0075-4102. DOI: 10.1515/crll.2003.043. URL: <http://dx.doi.org/10.1515/crll.2003.043>.
- [Fal03] Kenneth Falconer. *Fractal Geometry*. John Wiley & Sons Ltd, West Sussex, England, 2003.
- [Han56] Olof Hanner. “On the uniform convexity of  $L^p$  and  $l^p$ ”. In: *Ark. Mat.* 3 (1956), pp. 239–244. ISSN: 0004-2080.
- [Hei01] J. Heinonen. *Lectures on analysis on metric spaces*. Universitext. Springer-Verlag, New York, 2001, pp. x+140. ISBN: 0-387-95104-0. DOI: 10.1007/978-1-4613-0131-8. URL: <http://dx.doi.org/10.1007/978-1-4613-0131-8>.
- [HW41] Witold Hurewicz and Henry Wallman. *Dimension Theory*. Princeton Mathematical Series, v. 4. Princeton University Press, Princeton, N. J., 1941, pp. vii+165.
- [Hut81] John Hutchinson. “Fractals and self-similarity”. In: *Indiana Univ. Math. J.* 30.5 (1981), pp. 713–747. ISSN: 0022-2518. DOI: 10.1512/iumj.1981.30.30055. URL: <http://dx.doi.org/10.1512/iumj.1981.30.30055>.

- [KK] S. Keith and B. Kleiner. In preparation.
- [KL04] S. Keith and T. Laakso. “Conformal Assouad dimension and modulus”. In: *Geom. Funct. Anal.* 14.6 (2004), pp. 1278–1321. ISSN: 1016-443X. DOI: 10.1007/s00039-004-0492-5. URL: <http://dx.doi.org/10.1007/s00039-004-0492-5>.
- [Kig14] Jun Kigami. “Quasisymmetric modification of metrics on self-similar sets”. In: *Geometry and Analysis of Fractals*. Springer, 2014, pp. 253–282.
- [Kov06] Leonid Kovalev. “Conformal dimension does not assume values between zero and one”. In: *Duke Math. J.* 134.1 (2006), pp. 1–13. ISSN: 0012-7094. DOI: 10.1215/S0012-7094-06-13411-7. URL: <http://dx.doi.org/10.1215/S0012-7094-06-13411-7>.
- [KY92] Shigeo Kusuoka and Zhou Xian Yin. “Dirichlet forms on fractals: Poincaré constant and resistance”. In: *Probability theory and related fields* 93.2 (1992), pp. 169–196.
- [MT10] John Mackay and Jeremy Tyson. *Conformal dimension*. Vol. 54. University Lecture Series. Theory and application. American Mathematical Society, Providence, RI, 2010, pp. xiv+143. ISBN: 978-0-8218-5229-3.
- [Man67] Benoit Mandelbrot. “How Long Is the Coast of Britain? Statistical Self-Similarity and Fractional Dimension”. In: *Science* 156.3775 (1967), pp. 636–638. DOI: 10.1126/science.156.3775.636.
- [Mat95] Pertti Mattila. *Geometry of sets and measures in Euclidean spaces*. Vol. 44. Cambridge Studies in Advanced Mathematics. Fractals and rectifiability. Cambridge University Press, Cambridge, 1995, pp. xii+343. ISBN: 0-521-46576-1; 0-521-65595-1. DOI: 10.1017/CB09780511623813. URL: <http://dx.doi.org/10.1017/CB09780511623813>.
- [Mor46] P. Moran. “Additive functions of intervals and Hausdorff measure”. In: *Proc. Cambridge Philos. Soc.* 42 (1946), pp. 15–23.
- [Pan89] P. Pansu. “Dimension conforme et sphère à l’infini des variétés à courbure négative”. In: *Ann Acad. Sci. Fenn. Ser. A I Math* 14 (1989), pp. 177–212.
- [Pia] Matias Piaggio. “On the conformal gauge of a compact metric space”. To appear in: *Ann. Sci. École Norm. Sup.*

- [Pia11] Matias Piaggio. *Jauge conforme des espaces métriques compacts*. PhD Thesis, Aix-Marseille Université, 2011. URL: <http://tel.archives-ouvertes.fr/tel-00645284>.
- [Pia14] Matias Piaggio. “Conformal dimension and canonical splittings of hyperbolic groups”. In: *Geometric and Functional Analysis* 24.3 (2014), pp. 922–945.
- [Sch93] Oded Schramm. “Square tilings with prescribed combinatorics”. English. In: *Israel Journal of Mathematics* 84.1-2 (1993), pp. 97–118. ISSN: 0021-2172. DOI: 10.1007/BF02761693. URL: <http://dx.doi.org/10.1007/BF02761693>.
- [Sed88] Robert Sedgewick. *Algorithms*. Addison-Wesley, Reading, Mass, 1988.
- [Tuk89] Pekka Tukia. “Hausdorff dimension and quasisymmetric mappings”. In: *Math. Scand.* 65.1 (1989), pp. 152–160. ISSN: 0025-5521.
- [Tys00] Jeremy Tyson. “Sets of minimal Hausdorff dimension for quasiconformal maps”. In: *Proc. Amer. Math. Soc.* 128.11 (2000), pp. 3361–3367. ISSN: 0002-9939. DOI: 10.1090/S0002-9939-00-05433-2. URL: <http://dx.doi.org/10.1090/S0002-9939-00-05433-2>.
- [TW06] Jeremy Tyson and Jang-Mei Wu. “Quasiconformal dimensions of self-similar fractals”. In: *Rev. Mat. Iberoam.* 22.1 (2006), pp. 205–258. ISSN: 0213-2230. DOI: 10.4171/RMI/454. URL: <http://dx.doi.org/10.4171/RMI/454>.